Title
Pharmacological Targeting of IRE1α Ameliorates Insulin Resistance Through Preservation of the Insulin Receptor Signaling Pathway

Author
Colon-Negron, Kevin A

Publication Date
2019

Peer reviewed|Thesis/dissertation

Pharmacological Targeting of IRE1α Ameliorates Insulin Resistance Through Preservation of the Insulin Receptor Signaling Pathway

by
Kevin A. Colon-Negron

DISSERTATION
Submitted in partial satisfaction of the requirements for degree of
DOCTOR OF PHILOSOPHY

in

Biochemistry and Molecular Biology

in the

GRADUATE DIVISION
of the
UNIVERSITY OF CALIFORNIA, SAN FRANCISCO

Approved:

DocuSigned by:
Feroz Papa
9DCF56288A7E427...

Feroz Papa
Chair

DocuSigned by:
Kaveh Ashrafi
DocuSigned by:
Suneil Koliwad
DocuSigned by:
Robert Edwards
91579E192F544AF...

Kaveh Ashrafi
Suneil Koliwad
Robert Edwards

Committee Members

ACKNOWLEDGEMENTS

I have numerous people to thank for their support and help throughout these past 6 years in graduate school. First, I would like to thank my professor, Feroz Papa, for the provided financial support and mentoring. My thesis committee was an invaluable resource for me during this time and I thank Kaveh Ashrafi, Suneil Koliwad, and Robert Edwards for their mentorship and guidance throughout this process.

Next, I would like to thank the members of the Papa lab that I worked with for the past years including Alina Olivier, Rajarshi Ghosh, Maike Thamsen, and Likun Wang. I would like to point out Aeid Igbaria, who, more than helping me design and troubleshoot experiments for my thesis, was an exceptional example of a mentor to me. The scientist that I am today is largely because of his guidance and for always believing that I could perform good science. I am lucky to have had such an amazing team that assisted me with thoughtful discussion and technical issues in the lab.

In addition to the Papa lab, I am also beyond grateful to my very special friends Keyla Badillo, Eugenia Salcedo, Juan Caraballo, and José Cruz. They picked me up in my toughest and darkest moments of these last years and always reminded me that life needs to be lived and enjoyed to the fullest. You all are the best friends anyone could ever ask for. Thank you for making me part of your lives.

I would also like to thank God for all the talent He has given me. More importantly, for finding a way to let me know that I am loved and appreciated. I know it was You who, one way or another, got me through all this process.

Finally, I would like to dedicate my thesis to my parents, Inés Negrón (mami) and Jaime Colón (papi), and to my sister, Keyla Colón. I could not have done it without your

support in every single step of the way. I am everything that I am today because of you, but I am not even half of what you are. The hardest part of these past six years was not having you close to me. Papi, mami, Keyla: los amo con todo mi corazón. Gracias por su ayuda y amor incondicional. ¡Por fin temenos el primer Doctor de la familia!

Parts of chapter 1 of this thesis/dissertation/manuscript are a reprint of the material as it appears in *Cell Metab 2017*, 25(4):883-897 e888. The coauthors listed in this publication directed and supervised the research and experiments that were included in this dissertation/thesis.

Pharmacological Targeting of IRE1α Ameliorates Insulin Resistance Through Preservation of the Insulin Receptor Signaling Pathway

Kevin A. Colón-Negrón

ABSTRACT

Type 2 Diabetes (T2D) is characterized by a combination of factors that ultimately lead to loss of glycemic control. These factors include insulin resistance in insulin-responsive tissues (liver, muscle, and adipose tissues), and a progressive decline in β-cell mass and function. In addition, more than half of T2D patients are obese and more than 85% are overweight, which in turn contribute to the observed insulin resistance. It has been reported that obesity induces Endoplasmic Reticulum (ER) stress, which leads to peripheral insulin resistance and ultimately to T2D, yet the underlying mechanisms are not well understood. Using two different mouse models, we found that obesity and a high fat diet induces activation of the bifunctional ER transmembrane kinase/endoribonuclease (RNase)–IRE1α– and subsequent insulin desensitization by blunting phosphorylation of AKT. A mono-selective kinase inhibitor that allosterically attenuates IRE1α's RNase activity–KIRA8– prevented hyperglycemia, restored systemic insulin sensitivity, improved blood glucose clearance, enhanced insulin response in the liver and adipose tissues, and preserved pancreatic β-cell mass. Using chemical genetics tools of IRE1α we demonstrate that hyperactivation of IRE1α is sufficient to disrupt the insulin receptor signaling pathway. Our results demonstrate the potential efficacious properties of targeting IRE1α to enhance the adaptive capacity of the ER and prevent both peripheral insulin resistance and pancreatic β-cell loss.

TABLE OF CONTENTS

LIST OF FIGURES

LIST OF TABLES

INTRODUCTION

Diabetes mellitus is a group of metabolic disorders characterized by the body's inability to produce (type 1 diabetes) or respond (type 2 diabetes-T2D) to insulin, which is a hormone that is synthesized and secreted by the pancreatic β-cells in response to different stimuli (Fu, Gilbert et al. 2013). According to the Unites States Center for Disease Control (CDC), more than 30 million Americans had diabetes in 2018 and the diagnosed diabetes cost for America that same year was $327 billion. Moreover, these numbers are expected to increase in the next few years as 84 million Americans were diagnosed with prediabetes in 2018. Most of these patients with prediabetes are insulin resistant, a state that precedes the development of T2D (Mahat, Singh et al. 2019). Although T2D has been associated with obesity (Bays, Chapman et al. 2007), the molecular mechanisms by which obesity triggers T2D remain unclear.

Obesity and a high fat diet are major risks factors for the development of T2D as they cause the disruption of essential signaling pathways in peripheral insulin-responsive tissues (e.g. liver, adipose tissue, and muscle). The disruption of these signaling pathways interferes with the tissues' capacity to sense and properly respond to insulin, a condition known as insulin resistance. To compensate for insulin desensitization, pancreatic β-cells increase their workload in order to produce more insulin. Failing to fulfill the high insulin production demand, pancreatic β-cells undergo premature cell death, resulting in the pancreas' inability to produce enough insulin to overcome the cells' resistance (Butler, Janson et al. 2003, Del Guerra, Lupi et al. 2005). Consequently, patients exhibit elevated blood glucose levels (hyperglycemia) and, ultimately, become diabetic. Therefore, a solid understanding of the signaling pathway that leads to insulin

resistance in peripheral tissues and its link to diabetes is crucial to design effective therapeutic interventions for insulin resistance and T2D.

Insulin, as well as proteins in the secretory pathway, enter the Endoplasmic Reticulum (ER) where they undergo post translational modifications and structural maturation (Gething and Sambrook 1990). In order to efficiently fold these proteins, the ER possesses specialized and unique molecular chaperones and other protein-modification enzymes that assist with protein maturation (van Anken and Braakman 2005). Proteins that are not folded properly are tagged and degraded by the 26S proteasome in a process known as ER-associated protein degradation (ERAD) as a way to ensure that only correctly folded proteins enter the process of protein trafficking for delivery to downstream compartments (Vembar and Brodsky 2008). Despite these mechanisms to safeguard the proper folding of proteins, genetic mutations, environmental disturbances and pathological stress conditions, such as obesity and a high fat diet, compromise folding and structural maturation of secretory proteins. In turn, this leads to the accumulation of unfolded or misfolded proteins in the ER lumen. Under these conditions of “ER stress”, the ER protein folding demand exceeds the capacity of the ER. In order to cope with the increase in the folding demand and restore cellular homeostasis, the cell activates a set of signaling pathways known as the Unfolded Protein Response (UPR). The goal of the UPR is to alleviate ER stress and restore homeostasis by decreasing the protein folding demand on the cell and by increasing the synthesis of chaperones involved in protein folding (Walter and Ron 2011). However, If ER stress is chronic or irremediable, these adaptive outputs are surpassed by destructive signals. We

will now discuss the outputs of the UPR, the proteins regulating this response, and the role of the UPR in cell degenerative diseases such as diabetes, more in depth.

Three ER-transmembrane sensors initiate the UPR

The UPR is regulated by three ER transmembrane sensor proteins that sense and monitor the protein folding status of the ER through their luminal domains: activating transcription factor-6 (ATF6), protein kinase RNA (PKR)-like ER kinase (PERK), and inositol requiring enzyme-1 (IRE1α). ER stress activate these proximal UPR sensors to initiate a response in an effort to restore homeostasis in the ER. Two main adaptive outputs ('A'-UPR) events characterize this response and can be summarized in two different, yet interlinked, negative feedback loops. One negative feedback loop occurs quickly and aims to decrease the influx of protein into the ER, whereas the other is a slow negative feedback loop that involves the synthesis of de novo mRNA and protein to increase the ER folding capacity (Trusina, Papa et al. 2008). If this adaptive response is successful, the reduction in unfolded proteins causes UPR signaling to wane as homeostasis is restored (Merksamer, Trusina et al. 2008).

Alternatively, if ER stress remains irremediably high and adaptive outputs are overwhelmed, the UPR instead maladaptively "overshoots", leading to cell cycle arrest, dedifferentiation, senescence, sterile inflammation, and ultimately to cell death (Zhang and Kaufman 2006). The spectrum of these destructive outputs is called the terminal UPR ('T'-UPR). These adaptive and terminal outputs are mediated by the ER-transmembrane sensors ATF6, PERK, and IRE1α.

ATF6 is a 90kDa type II single pass transmembrane protein responsible for ER expansion and increased transcription of chaperones, foldases, and components of the ERAD pathway during ER stress (Adachi, Yamamoto et al. 2008, Bommiasamy, Back et al. 2009). In response to ER stress, the two different isoforms of ATF6, ATF6α and ATF6β, translocate from the ER to the Golgi, where they are cleaved by two serine-proteases (S1P and S2P) to generate a 50kDa active basic-leucine zipper (bZip) transcriptional factor (ATF6-N) (Ye, Rawson et al. 2000). ATF6-N is believed to act as an adaptive arm of the UPR that increases expression of chaperones and other enzymes through transcription of UPR target genes by binding to three different consensus sequences: (ERSE)-I (CCAAT-N9-CCACG/A), ERSE-II (ATTGG-N1-CCACG) and the UPRE (TGACGTGG/A) (Wang, Shen et al. 2000, Kokame, Kato et al. 2001).

PERK is a type I transmembrane protein that contains a cytosolic kinase domain that undergoes trans-autophosphorylation under ER stress. Upon activation, PERK phosphorylates the α-subunit of the eukaryotic translation initiation factor-2 (eIF2α). This event impedes subsequent rounds of translation initiation, resulting in the reduction of protein load in the ER lumen (Harding, Zhang et al. 1999, Harding, Zhang et al. 2000). While global translation is attenuated, phosphorylation of eIF2α promotes the selective translation of certain mRNAs. Such is the case for the mRNA encoding the transcription factor ATF4, which activates downstream UPR target genes (e.g., GADD34 and CHOP) that contribute to the enhancement of an antioxidant response and folding capacity of the ER (Harding, Novoa et al. 2000, Scheuner, Song et al. 2001). PERK is also associated with activating another transcription factor, NRF2, which also plays an important role in anti-oxidative response and mitochondrial bioenergetics demands (Harding, Zhang et al.

1999, Bobrovnikova-Marjon, Grigoriadou et al. 2010, Balsa, Soustek et al. 2019). Importantly, the levels of eIF2α phosphorylation are negatively controlled by two phosphatase complexes, the ER stress-inducible PPP1R15A/GADD34 (a target of ATF4/CHOP) and the constitutive phosphatase PPP1R15B/CReP (Hetz, Chevet et al. 2013). Interestingly, genes involved in apoptosis are a target of the transcription factor CHOP (Wang, Kuroda et al. 1998, Zinszner, Kuroda et al. 1998). Therefore, the PERK axis mediates a prosurvival response during the first stages of ER stress, but it switches into a proapoptotic response when ER stress remains unresolved.

The ER transmembrane sensor, IRE1, is the most ancient and conserved UPR component in eukaryotes (from yeast to humans), and it plays a major role in ER stress signaling (Zhang, Zhang et al. 2016). IRE1 is a type I trans-membrane protein that has a luminal domain that senses misfolded proteins and a cytosolic domain that is comprised of a bifunctional serine/threonine kinase and an endoribonuclease (RNase). Two different isoforms of IRE1 are found in mammalian cells, IRE1α and IRE1β. Although both of these isoforms share many similarities in their amino acid sequences and structures, they possess very different functions, which are primarily determined by their RNase domain (Tirasophon, Welihinda et al. 1998, Wang, Harding et al. 1998, Iwawaki, Hosoda et al. 2001, Imagawa, Hosoda et al. 2008). In this study we will focus only on IRE1α.

Upon ER stress, neighboring IRE1α monomers dimerize, and their kinase domains undergo trans-autophosphorylation. This event induces a conformational change of the RNase, allowing allosteric control of this domain. In turn, this causes the unconventional splicing of a 26-nt intron from the X-box binding protein-1 (XBP1) mRNA. Such cleavage will result in the generation of XBP1s (s=spliced) transcription factor, which increases

expression of genes that enhance ER protein folding and quality control such as ERAD, protein folding, chaperones, and lipid synthesis (Shen, Ellis et al. 2001, Yoshida, Matsui et al. 2001, Calfon, Zeng et al. 2002). Xbp1s target genes include: RAMP4, EDEM, p58IPK, HEDJ,DnaJ/Hsp40-like genes, Erdj4 and protein disulfide isomerase-P5 (Lee, Iwakoshi et al. 2003, Acosta-Alvear, Zhou et al. 2007). If ER stress persists, the RNase of IRE1α relaxes and loses its tight specificity for XBP1, causing destabilization of different RNAs through endonucleolytic cleavage of ER-localized mRNAs encoding ER targeted proteins in a mechanism called Regulated IRE1α-Dependent Decay (RIDD) (Hollien and Weissman 2006, Hollien, Lin et al. 2009). More recently, it has been shown that hyperactivation of the RNase domain of IRE1α also mediates the endonucleolytic cleavage of micro RNAs (miRNAs) (Lerner, Upton et al. 2012, Upton, Wang et al. 2012, Maurel, Chevet et al. 2014).

Another pathway that operates in an IRE1α-dependent manner is mediated by the mitogen-activated protein kinase (MAPK) c-Jun NH2-terminal kinase (JNK). Depending on the cellular context, JNK signaling can promote either adaptation or apoptosis (Weston and Davis 2007). During ER stress, IRE1α interacts with tumor necrosis factor receptor-associated factor 2 (TRAF2) (Urano, Wang et al. 2000). This leads to the activation of apoptosis signal-regulating kinase 1 (ASK1), which then initiates a phosphorylation cascade resulting in JNK phosphorylation and activation (Nishitoh, Matsuzawa et al. 2002). Under acute ER stress, JNK may promote cell death, as there is evidence that JNK can phosphorylate and inhibit anti-apoptotic proteins such as Bcl-2, Bcl-XL, and Mcl-1 (Weston and Davis 2007). Collectively, these destructive outputs of IRE1α are termed

terminal-UPR ('T'-UPR) outputs. However, the precise consequences of these destructive outputs and other means by which IRE1α promotes damage remain unclear.

In summary, these stress sensors –ATF6, PERK, and IRE1α– promote protein-folding homeostasis in the ER by transiently halting protein translation and increasing folding capacity; however, chronic or prolonged ER stress results in a switch from homeostasis to destruction and apoptosis.

The role of the UPR activation in the progression of diabetes mellitus

IRE1α has been shown to be critical in the development and progression of type 1 diabetes. Specifically, previous reports have demonstrated that sustained activation of IRE1α's RNase causes the direct cleavage of the precursor of microRNA-17, which is an upstream regulator of thioredoxin-interacting protein (TXNIP) (Upton, Wang et al. 2012). This is turn leads to the upregulation of TXNIP in pancreatic β-cells and further activation of the NLRP3 inflammasome, resulting in the premature cell death of β-cells (Lerner, Upton et al. 2012). Interestingly, inhibition of IRE1α with a small molecule prevented both the upregulation of TXNIP and the activation of the NLRP3 inflammasome, preserving functional β-cell mass and reversing hyperglycemia and established diabetes in a type 1 diabetes mouse model (Lerner, Upton et al. 2012). Therefore, it has become clear in the last few years that IRE1α can be a therapeutic target in cell degenerative diseases, including diabetes. Even though it has been shown that IRE1α is also activated in different mouse models of T2D, its exact contribution and role in the development of insulin resistance and T2D has yet to be elucidated.

Multiple lines of evidence support the notion that ER stress plays an important role in the pathogenesis of T2D, contributing to insulin resistance and β-cell failure (Ozcan, Cao et al. 2004, Salvado, Palomer et al. 2015). A high fat diet and obesity induce ER stress in insulin-responsive tissues, which ultimately leads to insulin resistance. Specifically, ER stress suppresses insulin signaling through JNK activation (Ozcan, Cao et al. 2004), which may represent a point of convergence between aberrant IRE1α signaling and insulin resistance. Moreover, β-cells are subjected to increased ER stress levels due to the increment in their workload to produce and secrete more insulin. In different type 1 diabetes mouse models, increased ER stress levels are known to activate 'T'-UPR outputs of IRE1α, which are responsible for the premature death of β-cells (Lerner, Upton et al. 2012, Ghosh, Wang et al. 2014, Morita, Villalta et al. 2017). However, it still remains to be elucidated if this is the case in T2D.

Aberrant IRE1α signaling may contribute to peripheral insulin resistance and eventual development of T2D. The polypeptide hormone insulin binds to its receptor at the cell membrane, promoting downstream activation and phosphorylation of other proteins, culminating with glucose uptake into the cell. Insulin resistance occurs when this insulin receptor signaling pathway is disrupted, causing a reduction in the sensitivity to insulin. The pro-survival kinase that regulates conversion of glucose into glycogen, AKT, is one of the proteins that becomes phosphorylated in this pathway upon insulin stimulation. ER stress was shown to suppress insulin-induced AKT phosphorylation, thereby promoting hepatic gluconeogenesis and insulin resistance (Ozcan, Cao et al. 2004). Remarkably, IRE1α has been shown to be activated in this scenario. Although we know that ER stress and UPR activation –including IRE1α– are critical in the progression

of insulin resistance, the specific role and downstream mediators by which IRE1α may contribute to insulin signaling disruption and subsequent T2D is still poorly characterized.

Obesity-induced ER stress and subsequent UPR activation have been shown to blunt AKT phosphorylation and impair insulin signaling in hypothalamus, fat, muscle and liver (Manning 2010). It is well-known that glucotoxicity and lipotoxicity-induced ER stress contribute to dysfunction and death of insulin-producing β-cells in pancreatic islets (Robertson, Harmon et al. 2003, Robertson, Harmon et al. 2004, Sharma and Alonso 2014, Oh, Bae et al. 2018). We propose that peripheral insulin resistance, relative insulin insufficiency and consequent β-cell overwork cause a vicious cycle that ends with β-cell apoptosis and ultimately a reduction in β-cell functional mass. Previous work in our lab has shown that blocking the IRE1α arm of the UPR by targeting its kinase preserved β-cell mass in different mouse models of ER stress-induced diabetes (Ghosh, Wang et al. 2014, Morita, Villalta et al. 2017). Therefore, agents or drugs that prevent both β-cell loss and insulin resistance should have significant disease-modifying potential in T2D.

In the first chapter of this dissertation, our aim was to understand the *in vivo* contribution of IRE1α in two mouse models of insulin resistance and T2D: (1) the high fat diet-fed and the (2) genetically modified *ob/ob* mice. Animals received a dose with a specific ATP-competitive IRE1α inhibitor called Kinase Inhibitors RNase Attenuator (KIRAs). By using this mono-selective small drug, we demonstrated that IRE1α plays a pivotal role in the development of hyperglycemia, a defining characteristic of T2D, as well as in insulin sensitivity, β-cell function, and blood glucose clearance.

In the second chapter of this project, we showed that ER stress, UPR activation, and aberrant IRE1α signaling directly attenuate the insulin receptor signaling pathway.

Using different genetic chemical tools, we showed that chronic activation of IRE1α ameliorates phosphorylation of AKT Ser473, a key protein in the insulin receptor signaling pathway that contributes to regulation of glucose metabolism. These results were also recapitulated in liver and adipose tissue from different mouse models.

This study has made an invaluable contribution to our understanding of the cellular and molecular interactions governing ER stress-induced insulin resistance and diabetes. The finding that IRE1α activation controls AKT phosphorylation has marked the discovery of a key event of the UPR in the development of diabetes. Additionally, this work has evaluated the efficacy of targeting the IRE1α arm of the UPR as a potential treatment for T2D and possibly for other protein misfolding and degenerative diseases.

CHAPTER 1

Targeting IRE1α with a Small Molecule

Ameliorates Insulin Resistance and Prevents β-cell loss *in vivo*

CHAPTER 1

SUMMARY

Hyperglycemia, glucose intolerance, insulin resistance and reduction of the functional pancreatic β-cells mass to below a critical threshold are critical hallmarks of type 2 diabetes (T2D). Obesity and a high fat diet (HFD) have been associated with the induction of Endoplasmic Reticulum (ER) stress and subsequent insulin resistance in peripheral tissues. Yet, the exact players and underlying mechanisms by which ER stress leads to insulin resistance and subsequent development of T2D are still not well understood. ER stress activates intracellular signaling pathways that are mediated by three ER-transmembrane sensors–ATF6, PERK, and IRE1α, whose combined outputs are known as the Unfolded Protein Response (UPR). Here, we show evidence that inhibition of IRE1α with a small molecule in two different insulin resistant and T2D mouse models (*ob/ob* and HFD-fed mice) prevents hyperglycemia and improves insulin sensitivity. Moreover, we found that administration of the IRE1α inhibitor prevented T2D development and preserved functional β-cell mass in both mouse models. This study identifies a novel link between the UPR, obesity, insulin resistance and T2D.

INTRODUCTION

In general, insulin resistance is a state in which cells that are normally responsive to insulin, such as adipocytes, hepatocytes and myocytes, start ignoring the signal of insulin. Essentially, insulin is a hormone that regulates glucose levels in our bloodstream by promoting glucose absorption in cells. Given that cells are unable to take up glucose during insulin resistance, the cells respond by activating other mechanisms to ensure that they still receive the fuel they need in the form of glucose. In fact, it has been shown that gluconeogenesis, a metabolic pathway that consists in the de novo synthesis of glucose from other molecules (e.g. pyruvate), is upregulated during insulin resistance (Valenti, Rametta et al. 2008, Hatting, Tavares et al. 2018). Closely related to the development of insulin resistance is the dysregulation of hepatic lipid metabolism (lipogenesis) (Sanders and Griffin 2016). Also, many insulin resistant patients end up experiencing premature β-cell death. Actually, it is thought that insulin resistance in peripheral tissues subjects pancreatic β-cells to an increased workload to compensate for insulin desensitization. Over time, β-cells cannot keep up with this exhausting task resulting in their damage and apoptosis, a state known as type 2 diabetes (T2D).

The Unfolded Protein Response (UPR) has been implicated as one signaling pathway involved in insulin resistance and β-cell failure. Accumulation of unfolded proteins in the Endoplasmic Reticulum (ER)– a condition known as ER stress– activates the UPR. The etiology of different hormonal and chronic diseases, such as T2D, have been linked to the induction of ER stress and subsequent activation of the UPR. The UPR initially attempts to restore homeostasis by increasing folding capacity; however, if ER stress is not resolved, the UPR will eventually trigger destruction (Ron and Walter 2007).

Particularly, it was demonstrated that obesity and a high fat diet induce ER stress and activate the UPR in insulin-responsive tissues, such as liver and fat (Ozcan, Cao et al. 2004). Interestingly, chemical chaperones that promote the hydrophobic effects of proteins have been shown to improve insulin sensitivity and glucose intolerance (Ozcan, Yilmaz et al. 2006), presumably by easing chronic ER stress and alleviating UPR destructive outputs. Given that we don't know the specific substrates of chemical chaperones as they can target many proteins, the molecular mechanisms and exact players involved in this destructive process are yet to be elucidated.

The UPR is mediated by three ER transmembrane stress sensors that transduce different signals of the response. The most conserved sensor, IRE1α, is an ER-transmembrane protein with an N-terminal luminal domain that is in charge of sensing unfolded proteins and a bi-functional cytosolic domain comprised of a kinase and an endoribonuclease (RNase) domain (Tirasophon, Welihinda et al. 1998, Wang, Harding et al. 1998). Unfolded proteins in the ER cause the luminal domains of neighboring IRE1α monomers to homo-oligomerize, inducing trans autophosphorylation of the kinase domains. Consequently, this event allosterically induces a conformational change of the RNase domains and makes it active. Activated IRE1α unconventionally splices its main mRNA substrate X-box binding protein 1 (XBP1), leading to a frameshift and the translation of a potent homeostatic transcription factor, XBP1s (s=spliced) (Yoshida, Matsui et al. 2001, Calfon, Zeng et al. 2002), which upregulates genes encoding ER protein-folding and quality control components (Lee, Iwakoshi et al. 2003). We have called these outputs of IRE1α Adaptive-UPR ('A'-UPR). However, severe or prolonged ER stress induces sustained, high levels of kinase autophosphorylation, causing

extensive IRE1α oligomerization. Subsequently, IRE1α's RNase domain relaxes and loses specificity for XBP1 and degrades hundreds of ER-localized mRNAs and miRNAs, which finally leads to destructive or Terminal-UPR ('T'-UPR) outputs. (Han, Lerner et al. 2009, Hollien, Lin et al. 2009, Lerner, Upton et al. 2012, Ghosh, Wang et al. 2014). Altogether, IRE1α activation attempts to restore homeostasis; however, unresolved ER stress leads to a switch from homeostasis to destruction.

The objective of the present study was to determine the role and contribution of IRE1α in the etiology and progression of insulin resistance and T2D. We hypothesize that obesity-induced ER stress hyperactivates IRE1α in peripheral insulin-responsive tissues, leading to 'T'-UPR outputs that ultimately cause insulin resistance and development of T2D through 'T'-UPR-dependent apoptosis in pancreatic β-cells **(Fig. 1.1)**. Using two different mouse models of insulin resistance, our findings show that we can prevent and reverse hyperglycemia, improve glucose and insulin tolerance, and preserve functional β-cell mass when IRE1α is systemically inhibited with a small molecule.

RESULTS

KIRA8 is a mono-selective kinase inhibitor for IRE1α

We have previously identified different Kinase Inhibitors RNase Attenuators (KIRAs) candidates for IRE1α that have been successfully tested *in vitro* and in different mouse models without any side effect (Lerner, Upton et al. 2012, Wang, Perera et al. 2012, Ghosh, Wang et al. 2014, Morita, Villalta et al. 2017, Thamsen, Ghosh et al. 2019). Despite the encouraging results, some KIRAs also inhibit other kinases at micromolar concentrations, raising the possibility that the effects of KIRAs proceed partially through off target effects (Mahameed, Wilhelm et al. 2019). However, a mono-selective IRE1α inhibitor –compound 18 **(Fig. 1.2A)**– which possesses all the properties of a KIRA and will be referred to as KIRA8 henceforth, was described (Harrington, Biswas et al. 2015, Morita, Villalta et al. 2017). To determine the efficacy of KIRA8, we determined its oligomer to monomer ratio *in vitro* and tested its ability to block the RNase activity of IRE1α using a recombinant soluble human IRE1α mini-protein construct containing only the kinase/RNase domains called IRE1α*. Specifically, KIRA8 blocks IRE1α* oligomerization at different concentrations **(Fig. 1.2, B and C)**. Also, KIRA8 potently inhibits IRE1α* RNase activity against XBP1 splicing and Ins2 mRNA degradation in lower concentrations compared other KIRA candidates **(Fig. 1.2, D and E)**. Furthermore, we confirmed the monoselectivity of KIRA8 for IRE1α *in vitro*, noting that it has minimal inhibition on IRE1α's closely paralog, IRE1β (Morita, Villalta et al. 2017); while other kinases operating in the UPR, including PERK, are not inhibited by KIRA8 **(Fig. 1.2F)** (Morita, Villalta et al. 2017). Therefore, KIRA8 proved to be a promising and exquisitely

selective drug-like small molecule against IRE1α that can be used *in vitro* and *in vivo* without any known toxicity.

IRE1α inhibition protects BTBR*lep*$^{ob/ob}$ mice against obesity-induced hyperglycemia

Leptin is a hormone secreted by adipose cells that is encoded by the *leptin* gene and regulates energy balance by inhibiting hunger. Animals that bear a homozygous mutation in this gene (i.e. *ob/ob* mouse) are unable to detect satiety despite high energy stores. In this context, *ob/ob* mice are constantly experiencing hunger, resulting in obesity and subsequent development of insulin resistance and type 2 diabetes (T2D). Importantly, the severity of the phenotype is closely related to the background of the mouse. For instance, *ob/ob* mice in the C57BL/6J background display obesity but transient hyperglycemia and do not undergo β-cell failure. On the other hand, *ob/ob* mice in the BTBR background exhibit a strong phenotype of hyperglycemia, insulin and glucose intolerance, subsequent β-cell failure and ultimately develop T2D (Chen, Hui et al. 2008).

Elevated ER stress levels, including IRE1α activation, has been reported and studied in the genetically-modified obesity-induced insulin resistance and T2D mouse model *ob/ob* (Ozcan, Cao et al. 2004, Ozcan, Yilmaz et al. 2006). However, the exact contribution of IRE1α in the onset and progression of insulin resistance and T2D is still unclear. To evaluate the role of IRE1α in T2D, we used the *ob/ob* mice in the BTBR background, which we will be referring to as the BTBR*lep*$^{ob/ob}$ mice. The BTBR*lep*$^{ob/ob}$ mice become insulin resistant at four weeks of age, hyperglycemic around six weeks of age and start undergoing β-cell failure when they are about two months old **(Fig. 1.3)**. To

this end, we administered BTBR*lep*$^{ob/ob}$ mice with a daily dosage of 50 mg/kg of KIRA8, which has been previously shown to prevent and reverse high blood glucose levels in NOD mice (type 1 diabetes mouse model) (Morita, Villalta et al. 2017). Administration of KIRA8 to BTBR*lep*$^{ob/ob}$ mice via intraperitoneal (I.P.) injection prevented high random blood glucose levels and maintained those levels relatively similar to normoglycemic levels seen in the lean wild type (WT) controls (519.6 ± 36.6 mg/dL versus 208.9 ± 12.7 mg/dL in vehicle versus KIRA8-treated BTBR*lep*$^{ob/ob}$ mice at 35 days post injection, $p < 0.0001$) **(Fig. 1.4, A and B)**. Normal blood glucose levels in the BTBR*lep*$^{ob/ob}$ mice was evident at day 10 after treatment and was maintained for up to 4 weeks. Moreover, vehicle-treated BTBR*lep*$^{ob/ob}$ mice exhibited severe hyperglycemia upon administration of glucose (2 g/kg) and showed impaired glucose tolerance. KIRA8 treatment significantly improved glucose tolerance in BTBR*lep*$^{ob/ob}$ mice with no apparent effect in the WT animals **(Fig. 1.4C and Fig. S1.1A)**.

Surprisingly, these blood glucose effects were also accompanied by a marked difference in body weight of the KIRA8-treated BTBR*lep*$^{ob/ob}$ and WT mice **(Fig. S1.1, B and C)**. To rule out the possibility that the effects observed in blood glucose are due to these differences in body weight and different food intake, we subjected BTBR*lep*$^{ob/ob}$ mice to a pair-feeding study. Since KIRA8 affects food intake of these mice (data not shown), we measured food intake of the KIRA8-treated mice daily and provided the vehicle-treated mice with the same amount of food in order to match body weight among both cohorts. We reasoned that if KIRA8 has a specific effect in preventing hyperglycemia and improving blood glucose disposal, then vehicle-treated BTBR*lep*$^{ob/ob}$ mice should still exhibit high blood glucose levels and glucose intolerance even when their body weights

are matched to that of the KIRA8 cohort. Animal weight was successfully matched in WT and BTBR*lep*$^{ob/ob}$ mice treated with vehicle and KIRA8 **(Fig. S1.1, D and E)**. However, vehicle-treated mice still became hyperglycemic compared to KIRA8-treated animals and no significant differences were observed in the WT animals **(Fig. 1.4, D and E)**. In line with these findings, KIRA8 also improved glucose tolerance in the BTBR*lep*$^{ob/ob}$ mice with glucose disposal curves comparable to WT animals **(Fig. 1.4F and S1.1F)**. These data support a model where KIRA8 prevents hyperglycemia and has a direct effect on insulin-responsive tissues independently of body weight.

KIRA8 administration ameliorates insulin resistance phenotype and preserves functional β-cell mass in BTBR*lep*$^{ob/ob}$ mice

We next quantified the effect of IRE1α's inhibition with KIRA8 in whole-body insulin sensitivity by determining serum insulin levels and performing insulin tolerance tests (Upton, Wang et al.). Fasting serum insulin levels were reduced by more than twofold in the KIRA8-treated BTBR*lep*$^{ob/ob}$ mice **(Fig. 1.5A)**, an indication of insulin resistance of the vehicle-treated animals and suggesting that KIRA8 is working to prevent hyperglycemia by increasing the animals' sensitivity to insulin. In line with the GTT and serum insulin levels results, KIRA8 improved insulin-stimulated blood glucose disposal in the BTBR*lep*$^{ob/ob}$ mice, without having an apparent effect on insulin action in the WT animals **(Fig. 1.5B)**. The Homeostatic Model Assessment for Insulin Resistance (HOMA-IR) was calculated using fasting blood glucose levels and fasting serum insulin levels as previous reports (Grote, Groover et al. 2013). BTBR*lep*$^{ob/ob}$ mice treated with vehicle had a significant elevated HOMA-IR as compared to KIRA8-treated mice (304.1 ± 56.8 in

vehicle compared to 57.3 ± 15.5 in KIRA8) **(Fig. 1.5C)**. Altogether, these results provide evidence that KIRA8 significantly improves glucose intolerance and insulin resistance in BTBR*lep*$^{ob/ob}$ mice.

To further study the effects of KIRA8 treatment on the metabolic profile of BTBR*lep*$^{ob/ob}$ mice, we determined serum triglyceride levels and ketone concentrations in mice subjected to treatments for 35 days. Both triglycerides and ketone bodies have been reported to be elevated in humans with insulin resistance and in different diabetic mouse models (Tirosh, Shai et al. 2008, Hudkins, Pichaiwong et al. 2010, Mahendran, Vangipurapu et al. 2013, Kim, Jung et al. 2016). Triglycerides and ketones levels were higher in vehicle-treated BTBR*lep*$^{ob/ob}$ mice, suggesting that these mice are insulin resistant and potentially diabetic –a phenotype that is prevented by KIRA8 **(Fig. 1.5, D and E)**. Since ketone bodies are mostly formed when liver glycogen stores are depleted and, given their high content in serum from BTBR*lep*$^{ob/ob}$ mice, we reasoned that gluconeogenesis would be activated in the liver to compensate for the lack of glucose uptake. To assess hepatic gluconeogenesis, we performed Pyruvate Tolerance Tests (PTT) in vehicle- and KIRA8-treated BTBR*lep*$^{ob/ob}$ mice. If mice are not sensitive to insulin, then an injection of pyruvate during the fasting state should systemically elevate blood glucose levels due to utilization of pyruvate as the first substrate of the gluconeogenic pathway in the liver. As expected, fasted vehicle-treated BTBR*lep*$^{ob/ob}$ mice showed higher blood glucose levels after a pyruvate injection compared to KIRA8-treated animals **(Fig. 1.5F)**, indicating activation of gluconeogenesis in the liver of these animals. Furthermore, critical gluconeogenic genes such as those encoding phosphoenolpyruvate carboxykinase (PEPCK) and glucose 6-phosphatase (G6P) were significantly

upregulated in livers of BTBR*lep*$^{ob/ob}$ mice, while KIRA8 reduced relative mRNA levels of these factors **(Fig. 1.5G)**. Moreover, upregulation of essential lipogenic genes in the liver was also observed in vehicle-treated BTBR*lep*$^{ob/ob}$ mice, indicating hepatic de novo lipid synthesis, which is not evident in KIRA8-treated animals **(Fig. 1.5H)**. This line of evidence is supported by previous reports that showed that de novo lipid synthesis is affected by expression of XBP1 in the liver (Lee, Scapa et al. 2008).

A hallmark of T2D is a decline in functional β-cell mass, which we hypothesize occurs due to increased workload in pancreatic β-cells to compensate for peripheral insulin resistance **(Fig. 1.1)**. It has been established that BTBR*lep*$^{ob/ob}$ mice undergo functional β-cell loss (Chen, Hui et al. 2008). We analyzed β-cell mass by determining the percentage of the pancreatic area that stained positively for insulin in relation to the entire pancreatic area. The amount of insulin-positive islet areas remained significantly greater in KIRA8-treated BTBR*lep*$^{ob/ob}$ mice 35 days after injections **(Fig. 1.5I)**. These results are evidence that IRE1α plays a detrimental and important role in the onset and progression of insulin resistance and T2D and affirms for the efficacy of KIRA8 to prevent hyperglycemia, insulin intolerance and β-cell loss.

IRE1α inhibition reverses insulin resistance in mice fed with a high fat diet

Investigation of the efficacy of KIRA8 in the BTBR*lep*$^{ob/ob}$ mice led to prevention of hyperglycemia, improvement of insulin sensitivity, and preservation of β-cell mass **(Fig. 1.4 and 1.5)**. Due to the severity of the disease phenotype in the BTBR*lep*$^{ob/ob}$ mice, administration of KIRA8 to mice with established hyperglycemia did not reverse the phenotype, which we hypothesize is due to how fast these mice undergo β-cell failure.

Therefore, we decided to turn to another insulin resistant mouse model to (1) demonstrate that KIRA8's effects are not specific to the BTBR background and (2) to evaluate KIRA8's efficiency for reversing hyperglycemia and improving insulin action in a more physiological diabetic animal model. To address these challenges, we used the diet-induced obese (DIO) mice as another model of insulin resistance. Specifically, C57BL/6J mice fed with a high fat diet (HFD) exhibit obesity with mildly elevated blood glucose levels (~180-200 mg/dL) and impaired glucose tolerance. C57BL/6J mice were subjected to HFD for 10 weeks to induce hyperglycemia and obesity compared to mice fed with standard CHOW diet **(Fig. S1.2, A and B)**. We then started administering vehicle or KIRA8 to these animals daily via I.P. injections for 31 days.

Random blood glucose levels of C57BL/6J mice treated with vehicle or KIRA8 were monitored twice a week for 31 days in CHOW and HFD-fed mice. Even though vehicle-treated HFD-fed mice seemed to have slightly higher blood glucose levels than their KIRA8-treated counterparts, no statistical significance was achieved between the cohorts (data not shown). However, we observed changes in blood glucose disposal by doing GTTs in HFD-fed mice treated with KIRA8. To assess the effect of IRE1α inhibition on glucose tolerance, we performed GTTs at day 0 and at day 28 after treatment. While vehicle-treated animals did not show any changes in the GTTs, mice treated with KIRA8 were significantly different from the vehicle measured at 28 days post injections **(Fig. 1.6A)**. Similarly to the BTBR*lep*$^{ob/ob}$ mice, insulin sensitivity was improved in the KIRA8-treated HFD-fed mice as measured by the ITT assay **(Fig. 1.6B)**. Consistent with these results, insulin levels and the HOMA-IR score were both elevated in the vehicle-treated mice fed with HFD, whereas KIRA8 treatment markedly reduced insulin levels in the HFD

mice comparable to mice fed with standard CHOW diet **(Fig. 1.6, C and D)**. Thus, these data provide evidence that IRE1α plays a detrimental role in the onset and progression of insulin resistance and that the effects of KIRA8 on glucose and insulin intolerance are not specific to the BTBR background. Even though KIRA8-treated mice were still obese at the end of the treatment, more studies are required to better understand the differences in body weight between animals treated with vehicle and KIRA8 **(Fig. S1.2C)**.

DISCUSSION

Accumulating evidence has described chronic ER stress and further activation of the UPR as a molecular link between obesity, insulin resistance and the development of type 2 diabetes (T2D) in animals and humans (Ozcan, Cao et al. 2004, Puri, Mirshahi et al. 2008). In the current study, we identified the ER stress sensor IRE1α as a modulator of obesity-induced insulin resistance and T2D in two different mouse models. Selective inhibition of IRE1α with the drug-like small molecule KIRA8, protected BTBR*lep*$^{ob/ob}$ mice from hyperglycemia **(Fig. 1.4)**. Unexpectedly, we found that KIRA8 affects food intake (data not shown). However, KIRA8-treated mice still became obese and continued to gain weight steadily albeit slower than the vehicle-treated animals. Nonetheless, more studies need to be performed in order to reveal the exact mechanism by which KIRA8 treatment causes a reduction in appetite. It is possible that KIRA8 also exerts an effect in other tissues that control hunger, such as the hypothalamus. In fact, several reports in the last decade have linked ER stress and abnormal UPR activation in the hypothalamus with obesity- induced insulin resistance and T2D (Milanski, Degasperi et al. 2009, Cnop, Foufelle et al. 2012, Flamment, Hajduch et al. 2012, Volmer and Ron 2015). We cannot rule out the possibility that KIRA8 could also be used as a drug to control body weight.

Not only do our studies show that targeting IRE1α can restore normoglycemia in mice that are prone to developing T2D, but we have also shown that daily administration of KIRA8 to mice improved blood glucose disposal without affecting control animals. Interestingly, vehicle-treated mice became hyperglycemic and glucose intolerant even when serum insulin levels were abnormally high, indicating that the observed phenotype was due to impaired insulin action and not because of inability to produce insulin. In line

with improved glucose intolerance, pharmacological inhibition of IRE1α reduced insulin levels and improved responsiveness to insulin in the BTBR*lep*$^{ob/ob}$ and High Fat Diet (HFD)-fed mice. Yet, BTBR*lep*$^{ob/ob}$ mice that received KIRA8 showed reduced insulin levels and improved insulin responsiveness; however, these levels were not comparable to those seen in the control animals, suggesting the presence of a therapeutic window. Consistent with these data, calculation of the HOMA-IR score revealed the presence and extent of insulin resistance in the BTBR*lep*$^{ob/ob}$ mice.

Obesity in mice and humans is associated with alterations in hepatic gluconeogenesis and lipid metabolism. We have shown that small molecule agents that enhance ER function to cope with these alterations can provide a unique approach to manage metabolic abnormalities associated with obesity and insulin resistance. Specifically, inhibition of IRE1α with KIRA8 resulted in the resolution of hepatic lipogenesis and possibly restoration of hepatic glucose uptake, indicated by the results of thge Pyruvate Tolerance Test and reduction in the expression of both lipogenic and gluconeogenic genes in the liver.

Finally, we were able to show that treatment with KIRA8 also preserves functional β-cell mass in the BTBR*lep*$^{ob/ob}$ mice. This is strong evidence that KIRA8 actually prevents development of T2D, as β-cell failure is a hallmark of the pathogenesis in both humans and mice. However, future studies will be needed to determine is these outcomes are due to systemic KIRA8 improving insulin resistance in peripheral tissues, having a direct effect in β-cells, or a combination of both. Although IRE1α activation was initially employed to help cells adapt to a heightened insulin demand, we speculate that unresolved ER stress and prolonged activation of IRE1α are the cause of the disease due to the switch to

terminal UPR outputs of IRE1α. We showed here that targeting the IRE1α arm of the UPR had multiple effects in different tissues, especially those that are responsive to insulin. Still the correction of the β-cell mass can be explained either by the ability of KIRA8 to inhibit the terminal outputs of IRE1α, or as direct result of a decrease in insulin demand and an improvement in insulin resistance. More experiments will be performed to investigate if KIRA8 also exerts some effects in pancreatic β-cells. We believe that targeting the UPR, specifically the IRE1α axis, with small molecules that alleviate destructive UPR outputs may warrant clinical investigation as a treatment for insulin resistance and T2D.

MATERIALS AND METHODS

In vitro IRE1α* Protein Preparation, Kinase, RNase and Crosslinking Assays

A construct containing the cytosolic kinase and RNase domains of human IRE1α (residues 469-977, IRE1α*) was expressed in SF9 insect cells using the Bac-to-Bac baculovirus expression system (Invitrogen) with a 6-His-tag at the N-terminus and purified with a Ni-NTA (QIAGEN) column. The RNase assay for the endpoint readings of IRE1α* (Figure 1.1D) was performed by using 50FAM-30BHQ-labeled XBP1 single stem-loop mini-substrate (50FAM- CUGAGUCCGCAGCACUCAG-30BHQ, from Dharmacon). For the endpoint readings of IRE1α* RNase activity, 0.1 mg/ml IRE1α* was incubated with 2 mM XBP1 mini-substrate for 20 min. Reaction mixtures were subsequently resolved by urea 15% PAGE. For the crosslinking experiments, IRE1α* was crosslinked with 250 mM disuccinimidyl suberate (DSS) (Sigma) in DMSO or 10 mM KIRA8 for one hr.

Kinome

KIRA8 was tested at a single dose at least in duplicate at a concentration of 1 μM against 365 kinases by Reaction Biology. Percent enzymatic activity was determined relative to DMSO-treated kinases. Curve fits were performed for KIRA8 when the remaining enzymatic activity was less than 65%.

Mouse Studies

Male BTBR*lep*$^{ob/ob}$ and C57BL/6J mice were obtained from the Jackson Laboratories (Stock numbers: 004824 and 000664, respectively). BTBR*lep*$^{ob/ob}$ mice were genotyped

by following the instruction of Jackson Laboratories. C57BL/6J mice were fed with high fat diet (Envigo; TD.88137) for 10 weeks starting at 6 weeks of age. Glucose levels were measured from tail snips obtained between 8:00 AM and 10:00 AM using a LifeScan glucose meter (OneTouch Ultra) twice per week. Diabetic mice were defined as having blood glucose levels of 250 mg/dL or above. All procedures were performed in accordance with protocols approved by the Institutional Animal Care and Use Committee at the University of California, San Francisco. Animals were kept in a specific pathogen-free animal facility on a 12 hr light- dark cycle at an ambient temperature of 21°C. They were given free access to water and food, except for the pair feeding experiment where vehicle-treated animals were pair-fed to KIRA8-treated animals.

Synthesis of KIRA8

*(S)-2-chloro-N-(6-methyl-5-((3-(2-(piperidin-3-ylamino)pyrimidin-4-yl)pyridin-2 yl)oxy)naphthalen-1-yl)benzenesulfonamide (KIRA8):*A solution of (S)-tert-butyl 3-((4-(2-((5-(2-chlorophenylsulfonamido)-2-methylnaphthalen-1-yl)oxy)pyridin-3- yl)pyrimidin-2-yl)amino) piperidine-1-carboxylate (4.36 g, 6.22 mmol) in DCM (15 ml) was treated with HCl in dioxane (3.5 M, 4 ml) and stirred at 50°C for 1 hr. The solution was then concentrated, and the remaining solid was triturated with Et_2O. Drying over P_2O_5 in a vacuum desiccator gave (S)-2-chloro-N-(6-methyl-5-((3-(2- (piperidin-3-ylamino)pyrimidin-4-yl)pyridin-2-yl)oxy)naphthalen-1-yl)benzenesulfonamide as an off-color and free-flowing solid (3.56 g, 90%). Product was determined to be 97.4% pure by reverse phase analytical chromatography (HPLC). ESI-MS: m/z = 601.3 $[M+H]^+$

(consistent with previously described characterization. Compound #18 in Harrington et al., 2014 (Harrington, Biswas et al. 2015)).

KIRA8 Treatments in BTBR*lep*$^{ob/ob}$ and HFD mice

Male BTBR*lep*$^{ob/ob}$ mice were randomized to KIRA8 or vehicle groups, and injected I.P. with KIRA8 (50 mg/kg) or vehicle (3% ethanol: 7% Tween-80: 90% saline) once a day, 5 times a week. 4-week-old BTBR*lep*$^{ob/ob}$ mice were used for prevention studies. Mice that were euthanized due to complication attributed to overt diabetes were excluded from the final analysis. In reversal studies in the C57BL/6J mice, KIRA8 (20 mg/dl) or vehicle treatment immediately commenced at week 11 after mice were exposed to high fat diet and continued for 4 weeks, 5 times a week. Blood glucose and body weight were monitored twice weekly. C57BL/6J mice were injected I.P. with KIRA8 or vehicle.

Glucose, Insulin, and Pyruvate Tolerance Tests

Mice were fasted for 6 hr before I.P. injection with glucose, insulin, or pyruvate. Blood was collected from the tail, and glucose levels were determined using LifeScan glucose meter (OneTouch Ultra). Concentrations of the reagents are specified in figure legends.

RNA Isolation, Quantitative Real-time PCR, and Primers

RNA was isolated from tissue using Trizol (Invitrogen). For standard mRNA detection, generally 1 μg total RNA was reverse transcribed using the QuantiTect Reverse Transcription Kit (QIAGEN). For qPCR, we used SYBR green (QIAGEN) and StepOnePlus Real-Time PCR System (Applied Biosystems). Thermal cycles were: 5 min

at 95°C, 40 cycles of 15 s at 95°C, 30 s at 60°C. Gene expression levels were normalized to 18S rRNA. Sequences of primers used for qPCR can be found in Table1.1.

Insulin, triglycerides, and ketones determination

All measurements were performed after 6 hours fast of the animals. Serum insulin levels were detected by ELISA following manufacturer instructions (EMD Millipore; Cat. #: EZRMI-13K). Triglycerides and ketones were measured using with a commercial kit from Sigma (Cat. #: TR0100-1KT and MAK134-1KT).

Pancreatic Insulin-positiveβ-cell area determination

Pancreatic sectioning, staining and analysis were done as described previously (Puri, Roy et al. 2018). Briefly, whole pancreas in paraffin-embedded blocks from vehicle and KIRA8 treated mice were serially sectioned and sections were picked every 100 microns apart to exclude overlapping islets. Immunohistochemistry was performed using anti-insulin antibody (Cell Signaling Technology) and counterstaining with hematoxylin. Using Adobe Photoshop, the area of insulin-positive islets and total pancreatic tissue for every section was measured. The results were expressed as a percent of insulin-positive islets area over the total pancreas area.

Statistical Analysis

All statistical analyses were performed using GraphPad Prism version 8.1. Student's t test or one-way ANOVA were applied to determine statistical difference between two

groups. Data are presented as mean ± SEM $p < 0.05$ was considered significant throughout the study. P values: * < 0.05; ** < 0.01; *** < 0.001; N.S., non-significant

TABLE 1.1. List of primers used for qPCR used in mouse livers

Gene	Forward Primer	Reverse Primer
PEPCK	GTCACCATCACTTCCTGGAAGA	GGTGCAGAATCGCGAGTTG
G6P	AGGTCGTGGCTGGAGTCTTGTC	GTAGCAGGTAGAATCCAAGCG
Acc2	GGGCTCCCTGGATGACAAC	TTCCGGGAGGAGTTCTGGA
Dgat2	TTCCTGGCATAAGGCCCTATT	AGTCTATGGTGTCTCGGTTGAC
Scd1	AGATCTCCAGTTCTTACACGACCAC	GACGGATGTCTTCTTCCAGGTG
18s	GTAACCCGTTGAACCCCATT	CCATCCAATCGGTAGTAGGC

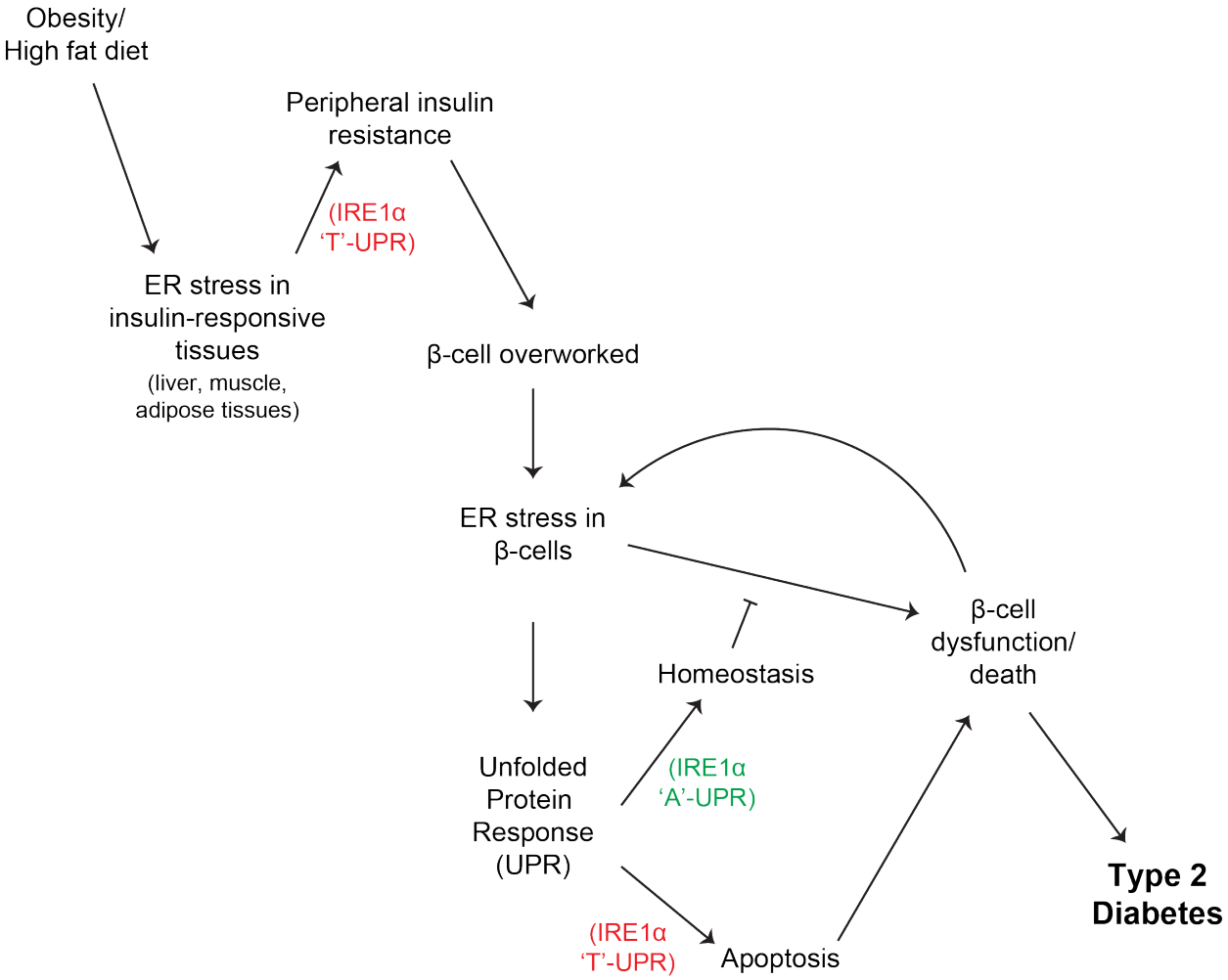

Figure 1.1. Conjectural scheme for a central role of ER stress and divergent UPR signaling in type 2 diabetes.

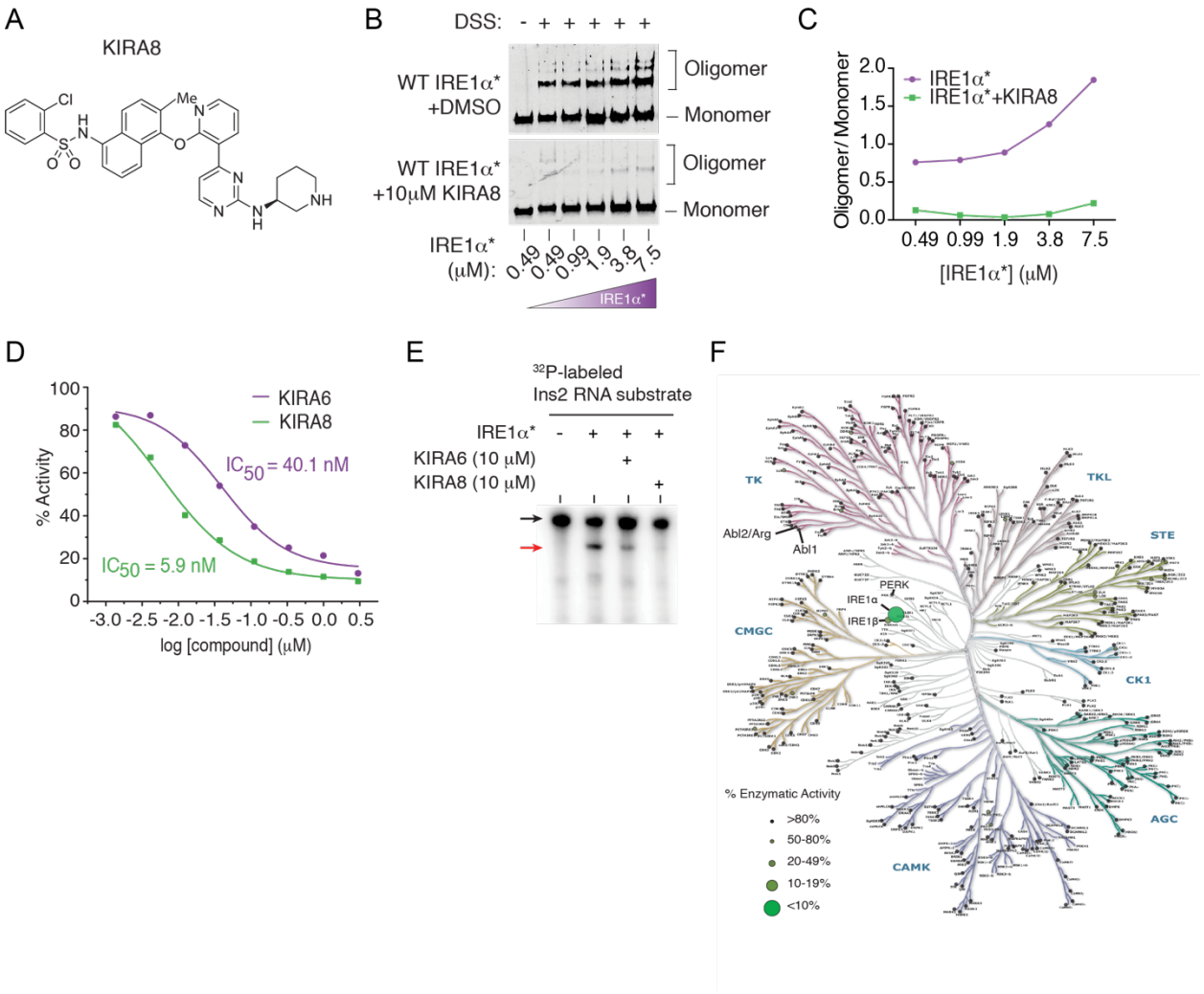

Figure 1.2. KIRA8 is a mono-selective drug-like small molecule for IRE1α that allosterically inhibits its catalytic activities.
(A) Structure of KIRA8.
(B) Western blots analysis of DSS-crosslinked varying [IRE1α*] ± KIRA8.
(C) Quantified oligomer/monomer ratio.
(D) Percent IRE1α* RNase activity against XBP1 mini-substrate at indicated concentrations. IC_{50}: KIRA6, 40.1 nM; KIRA8, 5.9 nM.
(E) Cleavage of α^{32}P-labeled mouse Ins2 RNA by IRE1α* ± KIRA6 or KIRA8.
(F) Selectivity of KIRA8 against 365 kinases; 1 μM KIRA8 was tested for inhibition of each kinase in duplicate.

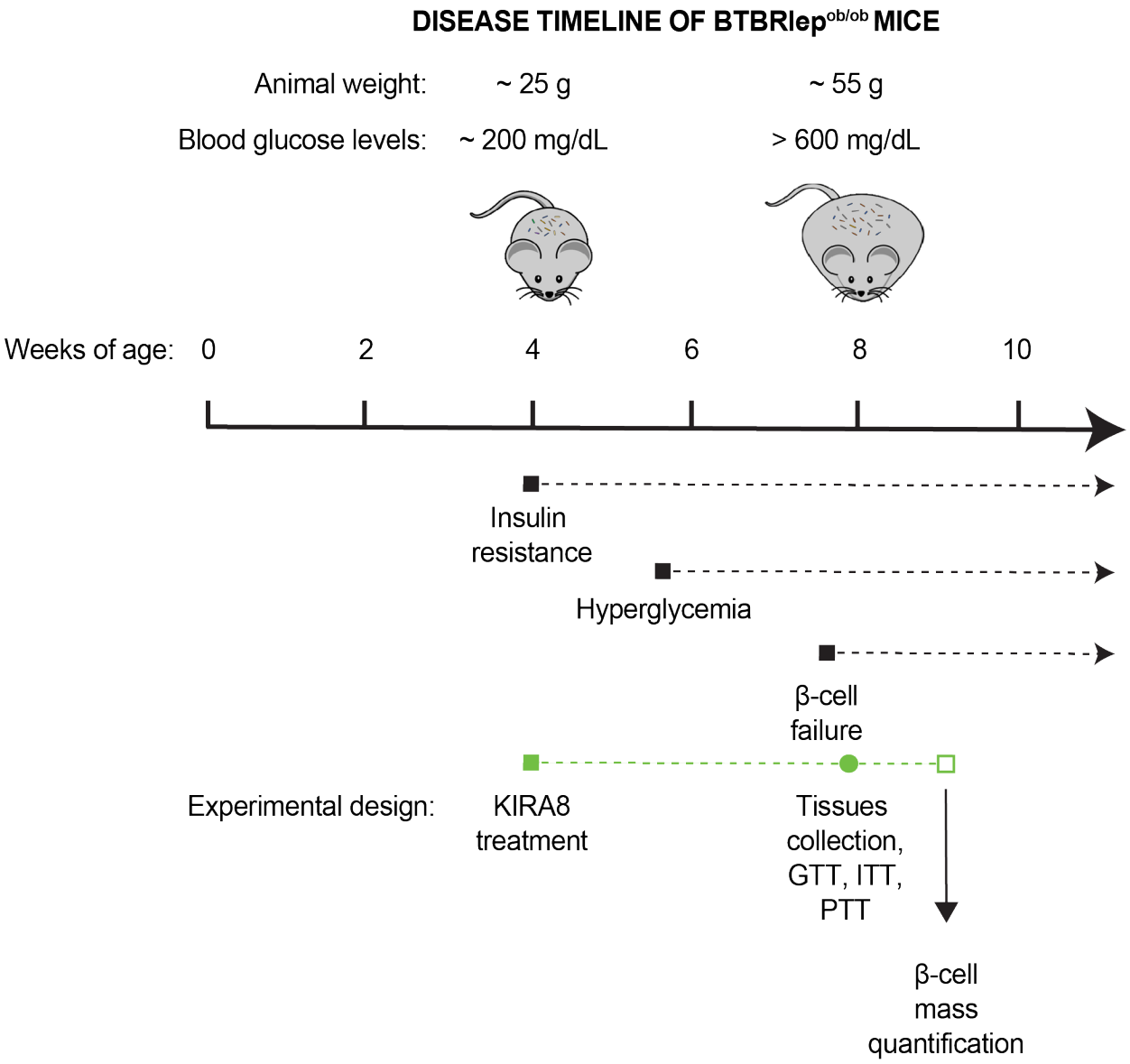

Figure 1.3. Timeline for the development of insulin resistance and type 2 diabetes in BTBR*lep*$^{ob/ob}$ mice.

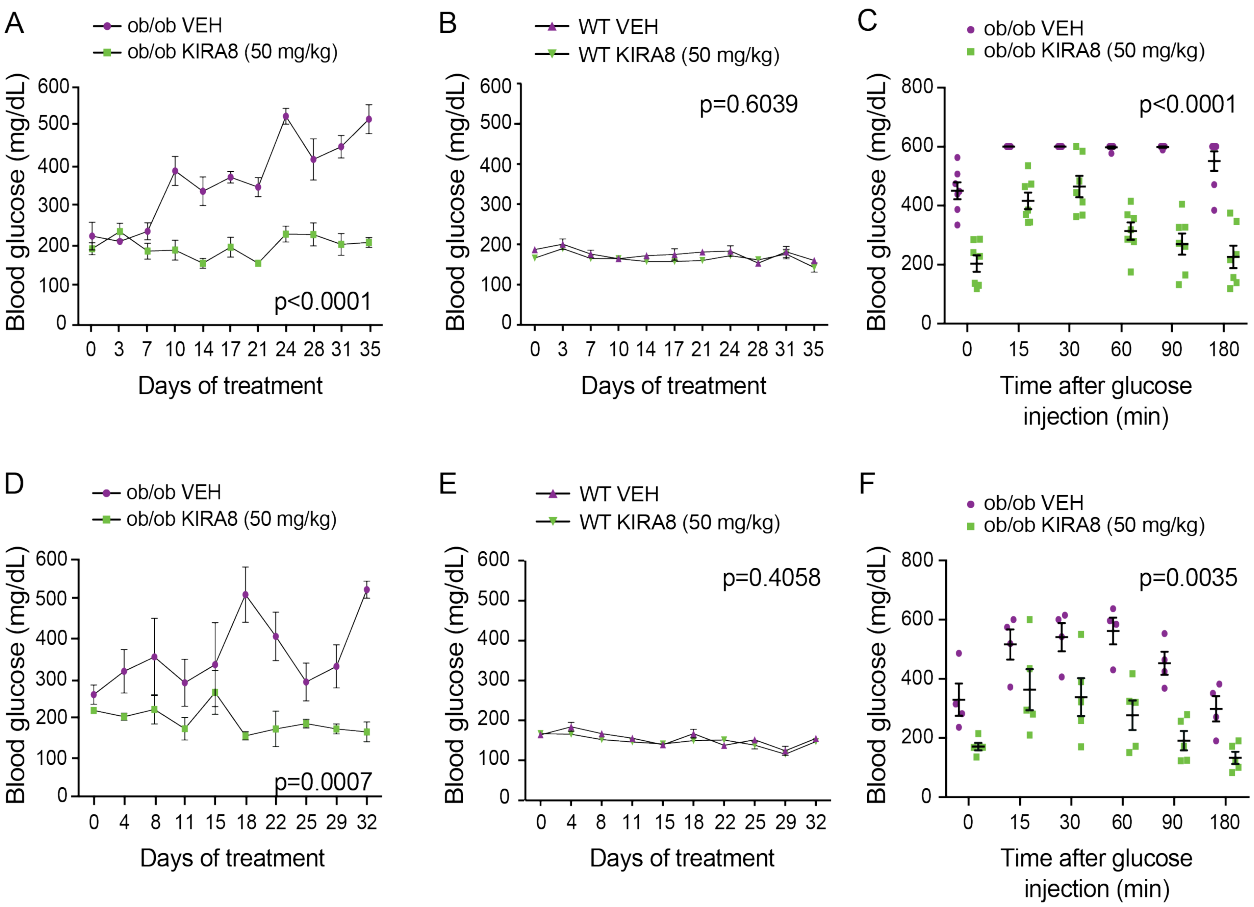

Figure 1.4. KIRA8 treatment prevents hyperglycemia and improves blood glucose disposal in the BTBR*lep*$^{ob/ob}$ mice.

(A) Random morning (AM) blood glucose (BG) levels in male BTBR*lep*$^{ob/ob}$ mice I.P. injected for 35 days once a day with KIRA8 (50 mg/kg) (n = 7) or vehicle (n = 7) starting at day 28 of age. BGs (mean ± SEM), analyzed by two-way RM ANOVA; $p < 0.0001$.

(B) Random AM BG levels in BTBR mice (WT males) subjected to same conditions as in (A). KIRA8 (50 mg/kg) (n = 4) or vehicle (n = 5). BGs (mean ± SEM), analyzed by two-way RM ANOVA; $p = 0.6039$.

(C) Glucose Tolerance Tests (GTT) on day 28 post injections. Male BTBR*lep*$^{ob/ob}$ mice were fasted for 6 hours and then I.P. injected with a glucose solution (2g/kg) (KIRA8 n = 7, vehicle n = 7). Each square shape represents an individual mouse. Two-way RM ANOVA; $p < 0.0001$.

(D) Random AM BG levels in male BTBR*lep*$^{ob/ob}$ mice subjected to a pair-feeding. Food intake of vehicle-treated animals (n = 4) was matched daily to their KIRA8 (50 mg/kg) counterparts (n = 5). BGs (mean ± SEM), analyzed by two-way RM ANOVA; $p = 0.0007$.

(E) Random AM BG levels in male WT BTBR mice subjected to same conditions as in (D) KIRA8 (50 mg/kg) (n = 5) or vehicle (n = 6). BGs (mean ± SEM), analyzed by two-way RM ANOVA; $p = 0.4058$.

(F) GTT on day 57 (29 days post injections) in pair-fed BTBR*lep*$^{ob/ob}$ mice after fasting for 6 hours. I.P. injection of (2 g/kg) glucose (KIRA8 n = 4, vehicle n = 5). Each square shape represents an individual mouse. Two-way RM ANOVA; p = 0.0035.

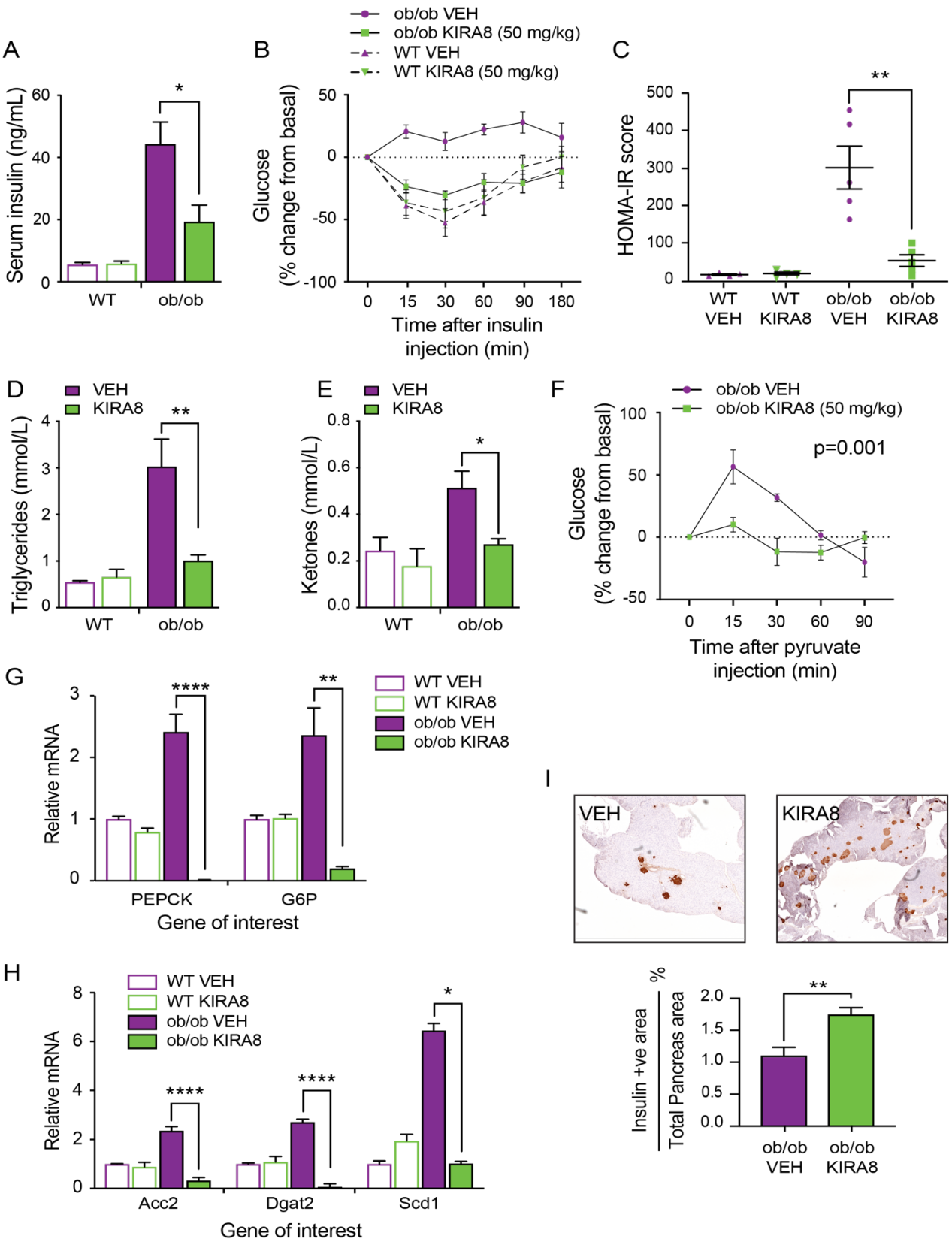
A
Serum insulin (ng/mL)
60
40
20
0
*
WT
ob/ob
B
ob/ob VEH
ob/ob KIRA8 (50 mg/kg)
WT VEH
WT KIRA8 (50 mg/kg)
Glucose (% change from basal)
50
0
-50
-100
0
15
30
60
90
180
Time after insulin injection (min)
C
HOMA-IR score
500
400
300
200
100
0
**
WT VEH
WT KIRA8
ob/ob VEH
ob/ob KIRA8
D
VEH
KIRA8
Triglycerides (mmol/L)
4
3
2
1
0
**
WT
ob/ob
E
VEH
KIRA8
Ketones (mmol/L)
0.8
0.6
0.4
0.2
0.0
*
WT
ob/ob
F
ob/ob VEH
ob/ob KIRA8 (50 mg/kg)
Glucose (% change from basal)
100
50
0
-50
p=0.001
0
15
30
60
90
Time after pyruvate injection (min)
G
Relative mRNA
3
2
1
0
****
**
WT VEH
WT KIRA8
ob/ob VEH
ob/ob KIRA8
PEPCK
G6P
Gene of interest
H
Relative mRNA
8
6
4
2
0
****
****
*
WT VEH
WT KIRA8
ob/ob VEH
ob/ob KIRA8
Acc2
Dgat2
Scd1
Gene of interest
I
VEH
KIRA8
Insulin +ve area / Total Pancreas area %
2.0
1.5
1.0
0.5
0.0
**
ob/ob VEH
ob/ob KIRA8

Figure 1.5. KIRA8 treatment enhances insulin responsiveness, decreases hepatic lipogenesis and gluconeogenesis, and preserves β-cell mass in BTBR*lep*$^{ob/ob}$ mice.
(A) Insulin levels in WT and BTBR*lep*$^{ob/ob}$ mice on day 56 (28 days post-injection) measured after 6 hours of fasting. KIRA8 (50 mg/kg) (n = 5) and vehicle (n = 4 – 5).
(B) Insulin (2 IU/kg) tolerance tests (Upton, Wang et al.) performed on day 56 (28 days post injections) in WT and BTBR*lep*$^{ob/ob}$ mice after fasted for 6 hours. Data are represented as the percent of change from the basal blood glucose levels at 0 min (KIRA8 n = 5 and vehicle n = 4 – 5). Two-way RM ANOVA; $p < 0.0037$.
(C) Homeostatic Model Assessment index for Insulin Resistance (HOMA-IR) in WT and BTBR*lep*$^{ob/ob}$ mice at day 56 (28 days post injections). Values were calculated using the equation $(G_0 \times I_0)/405$, where G_0 and I_0 are the fasting basal glucose and insulin levels, respectively (n= 4 – 5 animals in each group). Each symbol denotes an individual mouse.
(D and E) Triglycerides (D), and Ketones (E) levels in blood collected from 6 hours fasted WT BTBR and BTBR*lep*$^{ob/ob}$ mice 35 days after treatment. (KIRA8 n = 5 and vehicle n = 4 – 5). Bars represent means ± SEm. p values: * < 0.05, ** < 0.01.
(F) Pyruvate Tolerance Tests (PTT) on day 56 (28 days post injections) of 6 hours fasted BTBR*lep*$^{ob/ob}$ mice after challenged with 2 g/kg sodium pyruvate (KIRA8 n = 3, vehicle n = 4). Two-way RM ANOVA; $p < 0.0010$.
(G and H) Expression of gluconeogenic (G) and lipogenic (H) genes in liver of WT and BTBR*lep*$^{ob/ob}$ mice 28 days post injections was measured by quantitative real-time PCR with 18S ribosomal mRNA as control. Bars represent means ± SEm. p values: * < 0.05, ** < 0.01, *** < 0.001, **** < 0.0001.
(I) Total β-cell area as a percentage of total pancreas area on day 63 (35 days post injections). KIRA8 (50 mg/kg) (n = 6) and vehicle (n = 6).

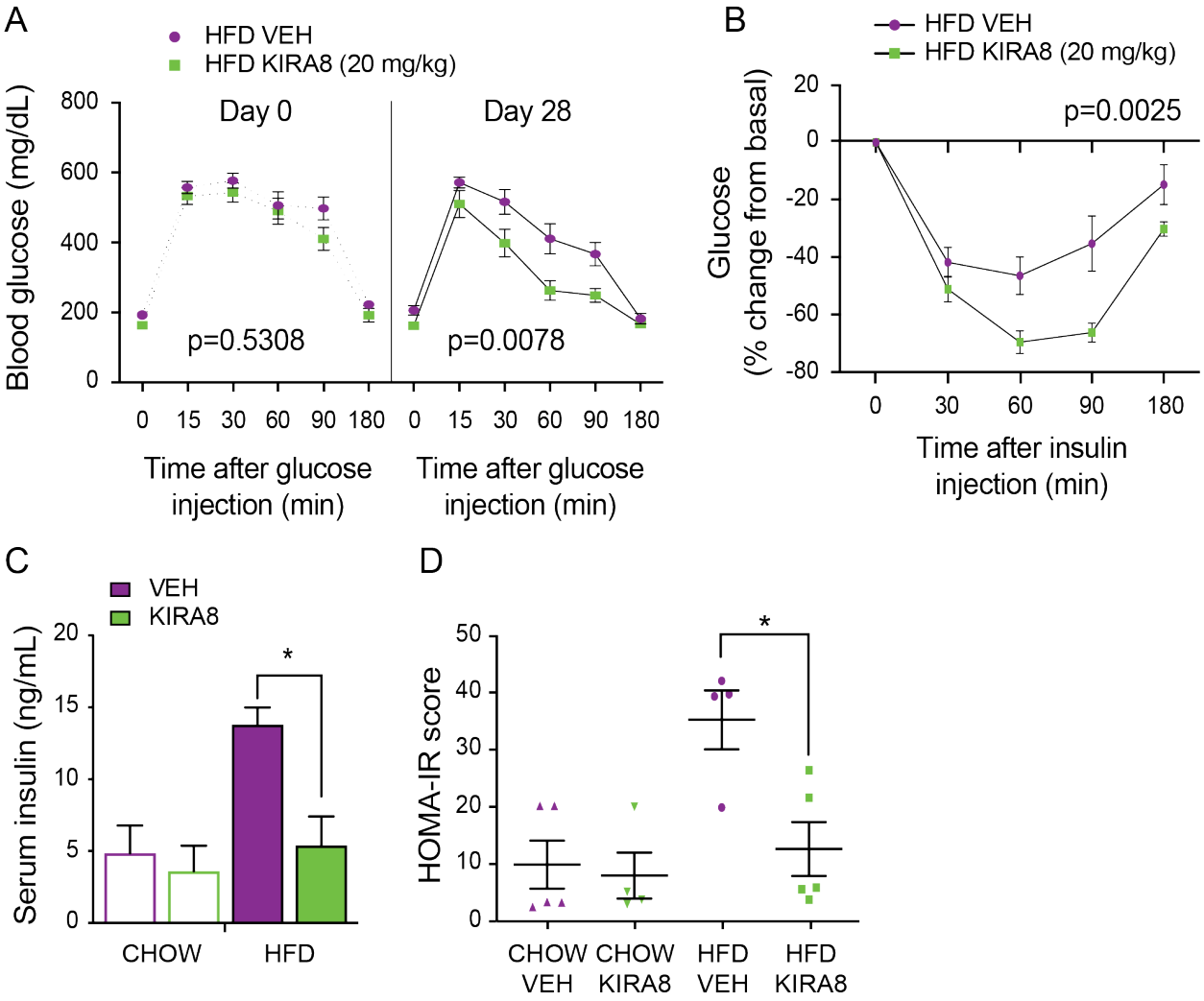

Figure 1.6. KIRA8 reverses established insulin resistance in C57BL/6J mice fed with high fat diet.

(A) GTT assays in vehicle- and KIRA8-treated mice (20 mg/kg) at day 0 and day 28 post injections. Mice were fasted for 6 hours before glucose injection (1 g/kg). n = 6 – 8 mice per group. Two-way RM ANOVA; day 0: p = 0.5308, day 31: p = 0.0078.

(B) Insulin Tolerance Test (Upton, Wang et al.) Assays (1 IU/kg), performed on day 28 post injections in 4-5 hours fasted CHOW and HFD mice. Data are represented as the percent of change from the basal blood glucose levels at 0 minutes (KIRA8 n = 7 and vehicle n = 6). Two-way RM ANOVA; p < 0.0025.

(C) Insulin levels in CHOW and HFD mice fasted for 6 hrs after 31 days of KIRA8 (20 mg/kg) or vehicle treatment. n = 4 – 5 mice/group.

(D) HOMA-IR in CHOW and HFD mice 35 days post injections. Values were calculated using the equation $(G_0 \times I_0)/405$, where G_0 and I_0 are the fasting basal glucose and

insulin levels, respectively (n= 4 – 5 animals in each group). Each symbol denotes an individual mouse.

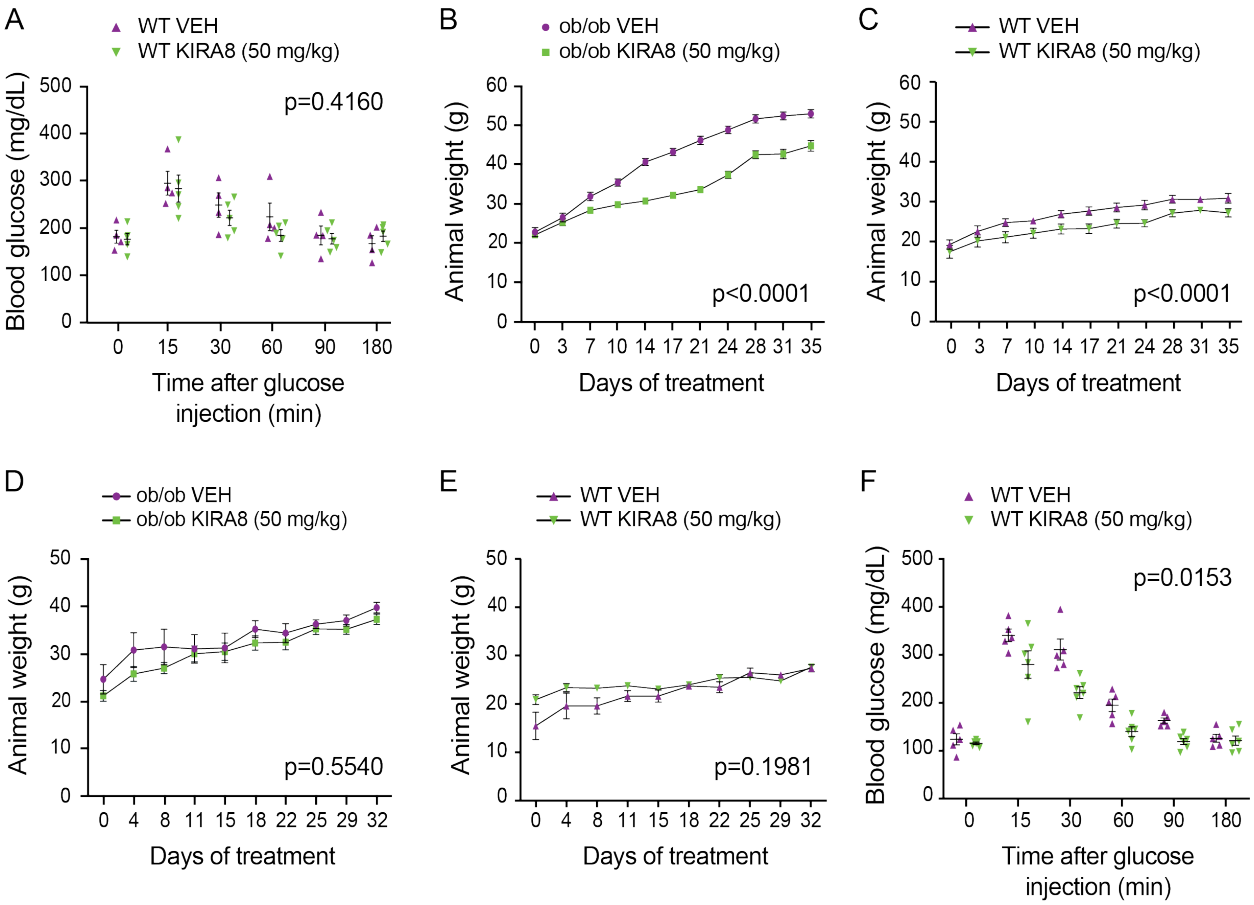

Figure S1.1. KIRA8 treatment affects body weight of BTBR*lep*$^{ob/ob}$ mice.
(A) GTT on day 56 (28 days post injections) after 6 hours fasting in WT mice from Figure 1.3B. I.P. injection of (2 g/kg) glucose (KIRA8 n = 4, vehicle n = 4). Each triangle shape represents an individual mouse. Two-way RM ANOVA; p = 0.4160.
(B and C) Cohort body weights of BTBR*lep*$^{ob/ob}$ (B) and WT (C) mice from Figures 1.1A and 1B, respectively. Two-way RM ANOVA; p < 0.0001 (BTBR*lep*$^{ob/ob}$) and p < 0.0001 (WT).
(D and E) Body weights of BTBR*lep*$^{ob/ob}$ (D) and WT (E) mice subjected to a pair-feeding study in Figures 1.1D and 1.1E, respectively. The animal weights of KIRA8- and vehicle-treated mice were successfully matched starting around day 11. Two-way RM ANOVA; p = 0.5540 (BTBR*lep*$^{ob/ob}$) and p = 0.1981 (WT).
(F) GTT on day 57 (29 days post injections) in pair-fed WT mice after fasting for 6 hours. I.P. injection of (2 g/kg) glucose (KIRA8 n = 6, vehicle n = 5). Two-way RM ANOVA; p = 0.0153.

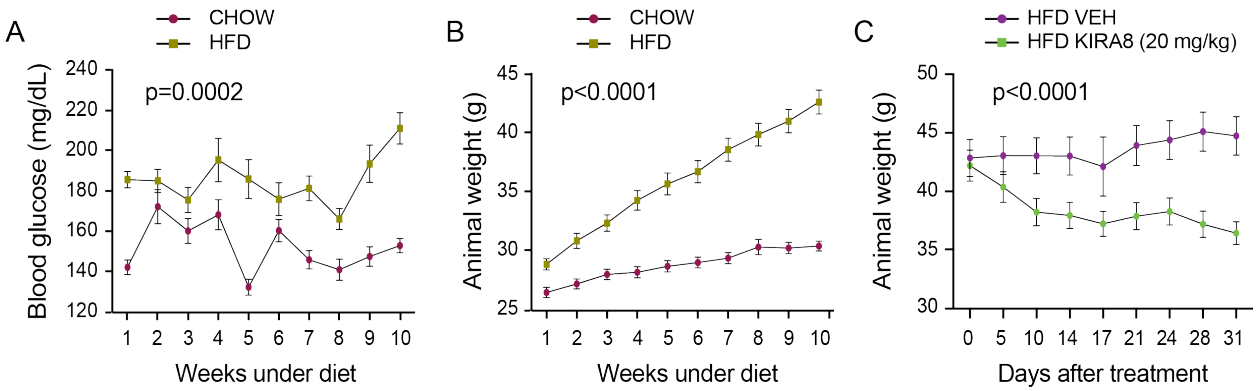

Figure S1.2. C57BL/6J mice developed hyperglycemia and became obese after being fed with High Fat Diet (HFD) for 10 weeks.
(A and B) Cohort random morning (AM) blood glucose (BG) levels (A) and body weights (B) of 6-weeks old C57BL/6J mice fed with regular CHOW (n = 14) or HFD (n = 14) for 10 weeks used in Figure 1.4. Two-way RM ANOVA; $p = 0.0002$ (BG) and $p < 0.0001$ (Body weight).
(C) Cohort body weights of vehicle- and KIRA8-treated mice that were fed with HFD. Two-way RM ANOVA; $p < 0.0001$.

CHAPTER 2

IRE1α is Both Sufficient and Necessary to Disrupt the Insulin Receptor Signaling Pathway and Prevent Glucose Uptake

CHAPTER 2

SUMMARY

Accumulation of unfolded proteins in the Endoplasmic Reticulum (ER) lumen, known as ER stress, activates signal transduction pathways, collectively known as the Unfolded Protein Response (UPR), that simultaneously transmits survival and apoptotic signals. Obesity and a high fat diet (HFD) have been shown to activate these responses in peripheral insulin-responsive tissues (i.e. liver, fat, muscle) of animals that are prone to developing insulin resistance. Yet, the exact contribution of these binary cell fate outcomes of the UPR to the development of obesity, HFD-induced insulin resistance and type 2 diabetes (T2D) have not been investigated. One of the proteins mediating the UPR, IRE1α, is a bifunctional kinase/endoribonuclease (RNase) that has been reported as a critical UPR life-death switch that functions as a “rheostat” to determine cell fate. Here, we show that terminal-UPR markers of IRE1α are upregulated in insulin-responsive tissues in an insulin resistant and T2D mouse model. Using chemical tools, we also found that destructive outputs of IRE1α are necessary and sufficient to disrupt the insulin receptor signaling pathway, converging at the phosphorylation of AKT. KIRA8, which is a small molecule that mono-selectively targets and inhibits IRE1α, reduced levels of UPR markers and re-sensitized animals and cells to insulin, as measured by AKT phosphorylation. This data indicates that IRE1α can be a potential therapeutic target for the treatment of chronic diseases such as insulin resistance and T2D.

INTRODUCTION

Insulin resistance is the result of the disruption of the insulin receptor signaling pathway. After a meal, blood glucose levels rise and, in response, the pancreas releases insulin for glucose uptake in the insulin responsive tissues. Specifically, insulin in the extracellular space binds the insulin receptor in the plasma membrane with an affinity in the picomolar range (Whittaker, Hao et al. 2008). This interaction results in the phosphorylation of the insulin receptor substrate (IRS) by the insulin receptor. Phosphorylated IRS recruits the phosphoinositide 3-kinase (PI3K) to the plasma membrane, which catalyze the production of phosphatidylinositol-3, 4, 5-triphosphate (PIP3) by phosphorylating phosphatidylinositol-4, 5-bisphosphate (PIP2). PIP3 now serves as a platform for the binding of the Pyruvate Dehydrogenase Kinase 1 (PDK1) at the plasma membrane. PDK1 recruits and phosphorylates the pro-survival protein kinase B (PKB; also known as AKT) at the Thr308. In order for AKT to be fully activated, the multiprotein complex mTORC2 needs to phosphorylate AKT at Ser473 (Alessi, Caudwell et al. 1996, Klippel, Kavanaugh et al. 1997, Sarbassov, Guertin et al. 2005). This critical phosphorylation event can be useful for investigating the activation of the insulin receptor signaling pathway, as it is a measurement of insulin sensitivity. The phosphorylation of AKT activates a signaling cascade that involves the phosphorylation of multiple proteins, which culminates in the translocation of the glucose transporter 4 (GLUT4) from the cytosol to the plasma membrane. At the cell surface, GLUT4 permits the absorption of glucose, which now is used by the cell as a source of energy **(Fig. 2.1)**. In turn, this allows the restoration of normoglycemia and, as a consequence, insulin levels in the blood drop.

ER stress has been shown to disrupt the insulin receptor signaling pathway both *in vivo* and *ex vivo*. Specifically, different chemical agents that induce ER stress, such as the N-glycosylation inhibitor Tunicamycin (Tm) and the saturated fatty acid palmitate (Palm), suppress insulin-stimulated AKT Ser473 phosphorylation in different cell lines (i.e. hepatocytes, adipocytes, myocytes), suggesting that chemically-induced ER stress plays a detrimental role in the disruption of the insulin receptor signaling pathway (Ozcan, Cao et al. 2004, Koh, Toyoda et al. 2013). Moreover, AKT Ser473 phosphorylation has been shown to be blunted due to ER stress induced by obesity or high fat diet in different mouse models. In line with these data, insulin-stimulated glucose uptake is reduced in cells exposed to ER stress, suggesting the development of insulin resistance. In fact, previous reports have demonstrated that treatment with chemical chaperones that promote the hydrophobic effects of proteins and, thus, alleviate ER stress, improves insulin sensitivity and restore normoglycemia in an insulin resistance mouse model (Ozcan, Yilmaz et al. 2006). Even though IRE1α has been shown to be activated in these conditions, the specific mechanism by which IRE1α interferes with the insulin receptor signaling pathway is not well understood.

The objective of this investigation is to demonstrate the link between the insulin receptor signaling pathway and ER stress, specifically IRE1α activation. Here we provide evidence that IRE1α hyperactivation is necessary and sufficient to blunt AKT Ser473 phosphorylation, a key event in the insulin receptor signaling pathway. Moreover, we demonstrate that treatment with KIRA8, a mono-selective IRE1α inhibitor, alleviates obesity-induced ER stress markers in liver and adipose tissues while enhancing insulin responsiveness simultaneously in both tissues.

RESULTS

KIRA8 treatment reduces ER stress markers and restores AKT Ser473 phosphorylation in liver and adipose tissues of BTBR*lep*$^{ob/ob}$ mice

Amelioration of ER stress with chemical chaperones in obese mice has been associated with improvement in glucose tolerance and insulin response (Ozcan, Yilmaz et al. 2006). We have previously shown that targeting IRE1α *in vitro*, as well as in different murine models, can ameliorate global ER stress levels and restore homeostasis (Ghosh, Wang et al. 2014, Morita, Villalta et al. 2017, Thamsen, Ghosh et al. 2019). We hypothesized that if hyperglycemia, glucose intolerance, and insulin resistance are the result of elevated ER stress levels in peripheral insulin-responsive tissues, then IRE1α inhibition with KIRA8 treatment should reduce expression of ER stress markers and restore insulin sensitivity in the BTBR*lep*$^{ob/ob}$ mice. As expected, total XBP1 mRNA levels were higher in the livers of vehicle-treated BTBR*lep*$^{ob/ob}$ mice, as were levels of markers of terminal UPR ('T'-UPR) activation: the transcription factors ATF4 and CHOP, and the ER-resident chaperone BiP. On the other hand, animals treated with KIRA8 showed a reduction in the relative mRNA levels of these genes, indicating amelioration of ER stress and 'T'-UPR markers **(Fig. 2.2A)**. These data correlate with a reduction in blood glucose levels and insulin levels, and an improvement in glucose tolerance, as Chapter 1 explored. Spliced XBP1 mRNA in the liver was more than 2-fold higher in BTBR*lep*$^{ob/ob}$ mice that were treated with vehicle in comparison to KIRA8-treated counterparts or wild types, indicating the presence of ER stress and confirming that KIRA8 targets IRE1α **(Fig. 2.2B)**. Similar results were obtained through analysis of adipose tissue, demonstrating

that KIRA8 operates systemically to reduce IRE1α activation in multiple insulin-responsive tissues **(Fig. S2.1A)**. ERdj4, one of the direct targets of the transcription factor XBP1s, was upregulated in the vehicle-treated BTBR*lep*$^{ob/ob}$ mice and is downregulated in the presence of KIRA8, further confirming our results for spliced XBP1 **(Fig. 2.2C)**. In line with our observations and other reports, such as those documented by Ozcan et al., phosphorylation of c-Jun was observed in the liver of the same group of BTBR*lep*$^{ob/ob}$ mice from Fig. 2.4A in Chapter 1, while treatment with KIRA8 reduced levels of c-Jun phosphorylation **(Fig. 2.2D)**. Consistent with reduction of ER stress markers, XBP1 protein levels were also lower in BTBR*lep*$^{ob/ob}$ mice that had been treated with KIRA8 **(Fig. 2.2D)**.

If our hypothesis that hyperactivation of IRE1α causes insulin resistance through disruption of the insulin receptor signaling pathway in peripheral tissues is correct, then inhibition of IRE1α with KIRA8 should reestablish the signaling capacity of insulin in liver and adipose tissue. To test this notion, we looked at phosphorylation of AKT at Ser473, a more distal event in the insulin receptor signaling pathway that culminates in the insulin-mediated uptake of glucose. Treatment with KIRA8 not only rescued AKT Ser473 phosphorylation, but it also lowered basal AKT phosphorylation levels of in the livers of BTBR*lep*$^{ob/ob}$ mice **(Fig. 2.2E)**. Similarly, insulin-stimulated AKT Ser473 phosphorylation was improved in adipose tissue of KIRA8-treated BTBR*lep*$^{ob/ob}$ mice **(Fig. S2.1B)**. Overall, these data suggest that KIRA8 ameliorates hyperglycemia and glucose intolerance by suppressing 'T'-UPR markers and enhancing systemic insulin action in peripheral tissues *in vivo*.

KIRA8 treatment restores AKT Ser473 phosphorylation in High Fat Diet fed C57BL/6J mice.

We successfully showed that inhibition of IRE1α with KIRA8 reverses insulin resistance and improves blood glucose disposal (GTT) in mice fed with high fat diet (HFD) (Chapter 1, Fig. 1.6). We then asked whether ER stress plays a role in the disruption of the insulin receptor signaling pathway and whether we can rescue AKT Ser473 phosphorylation with KIRA8 treatment. For this, we looked at ER stress markers in HFD fed-mice treated with vehicle or KIRA8. In mice that were treated with vehicle for 31 days, we observed higher levels of the relative mRNA of ATF4, CHOP, and BiP than in the KIRA8-treated animals; however, despite this pattern, no statistical significance was achieved between groups (data not shown). Nonetheless, when we tested the XBP1 splicing in the liver of these mice, we found that XBP1s is more abundant in the HFD fed-mice treated with vehicle compared to those treated with KIRA8 **(Fig. 2.3A)**. This indicates the presence of ER stress in the HFD-fed mice albeit to a lesser degree than in the BTBR*lep*$^{ob/ob}$ mice, which display a much more severe insulin resistance phenotype. In fact, just as observed in the BTBR*lep*$^{ob/ob}$ mice, KIRA8 enhanced insulin action in the livers of HFD fed-mice, as was demonstrated by phosphorylation of AKT at Ser473 **(Fig. 2.3B)**. Overall, these data are evidence that activation of IRE1α promotes attenuation of AKT Ser473 phosphorylation, while treatment with KIRA8 restores AKT Ser473 phosphorylation through suppression of the UPR.

Chemically-induced ER stress disrupts the insulin receptor signaling pathway through inhibiting of AKT Ser473 phosphorylation.

In order to evaluate the effect of ER stress on the insulin receptor signaling pathway, we turned to the human liver cell line HepG2, and the rat hepatocyte cell line H4IIEC3. HepG2 cells were starved for 24 hours in order to eliminate the effect of insulin found in the serum, and cells were subsequently subjected to different concentrations of insulin. We then monitored the phosphorylation of AKT at Ser473 as an indicator for AKT activation, and we found that 0.6 nM of insulin for 5 minutes is enough to increase AKT phosphorylation by ~2 fold **(Fig. S2.2A)**. We next investigated if the induction of ER stress with different chemical agents would prevent the phosphorylation of AKT at Ser473 upon insulin stimulation. Treatment of HepG2 cells for 24 hours with different concentrations of Tm, BFA and Palmitate prior to the addition of insulin, blunted AKT Ser473 phosphorylation in HepG2 cells in a concentration-dependent manner **(Fig. S2.2, B – D)**. We monitored total IRE1α levels in these conditions as an indication of Tm- and BFA-induced ER stress **(Figure S2.2, B-C)**.

We next investigated the potential of KIRA8 to rescue AKT Ser473 phosphorylation through inhibition of the IRE1α arm of the UPR in HepG2 cells during ER stress. Pre-treatment of the HepG2 cells with KIRA8 for 1 hour prior to ER stress induction increased the phosphorylation levels of AKT Ser473 compared to cells that were challenged with ER stress inducers in the absence of the inhibitor **(Fig. 2.4A)**. XBP1 splicing was reduced in the presence of KIRA8, confirming that the drug is targeting IRE1α **(Fig. 2.4B)**. To ensure that physiological effects of KIRA8 are general, and not restricted to a certain cell type, we also treated rat H4IIEC3 hepatocytes with Palmitate in the presence or absence

of KIRA8. Palmitate induced XBP1 mRNA splicing in H4IIEC3 cells and blunted insulin-stimulated AKT Ser473 phosphorylation, but KIRA8 rescued these events **(Fig. 2.4, C-D)**. Hence, ER stress disrupts the insulin receptor signaling pathway and inhibition of IRE1α with KIRA8 leads to improvement in insulin-induced AKT Ser473 phosphorylation independently of the cell type.

IRE1α's terminal-UPR outputs are required to blunt AKT Ser473 phosphorylation and reduce glucose uptake *in vitro*

To assess the exact contribution of IRE1α in the reduction of AKT Ser473 phosphorylation, we used previously generated T-REx293 cell lines with a doxycycline-inducible system that controls expression of either transgenic wild type IRE1α or different mutant versions of IRE1α **(Fig. S2.3, A and B)** (Han, Lerner et al. 2009). Upon induction with doxycycline (Dox), the transgenic IRE1α protein self-associates by mass action. In this context, transgenic IRE1α is activated without requiring upstream ER stress and without pleiotropic effects caused by other chemical agents that activate all axes of the UPR. Hence, these tools allow us to study the precise contribution of IRE1α to any physiological process that is linked to the UPR.

T-Rex293 cells expressing transgenic WT IRE1α were subjected to a treatment with Dox in FBS-free media for 48 hours, a regime that has been shown to promote 'T'-UPR outputs. Cells were then stimulated with 10 nM of insulin for 10 minutes to activate the insulin receptor signaling pathway. As expected, IRE1α is upregulated under these conditions, protein levels of spliced XBP1 and BiP were elevated, and the pro-apoptotic protein JNK was phosphorylated **(Fig. 2.5A)**. Using this system, we found that insulin-

stimulated AKT Ser473 phosphorylation was blunted under IRE1α overexpression, but KIRA8 restores this phosphorylation by inhibiting IRE1α activation, which was measured by determination of XBP1s protein levels **(Fig. 2.5B)**.

In order to study the contribution of the different outputs of IRE1α on AKT phosphorylation, we used different IRE1α mutants. We previously generated T-REx293 cells expressing a kinase mutant of IRE1α (I642G) **(Fig. S2.3B)** (Han, Lerner et al. 2009). This point mutation enlarges the adenosine triphosphate (ATP)-binding pocket in its kinase domain and severely compromise the phosphotransfer catalytic activities of IRE1α (Papa, Zhang et al. 2003, Han, Lerner et al. 2009). Due to its enlarged kinase pocket, IRE1α (I642G) can selectively bind the cell-permeable adenosine nucleotide mimic with a bulky chemical head group 1NM-PP1. By doing so, it can bypass the trans-autophosphorylation requirement and allosterically activates IRE1α's RNase domain, but only for XBP1 splicing without activating RIDD. That is, IRE1α (I642G) is partially activated upon 1NM-PP1 administration but only for adaptive outputs as it cannot surpass the oligomerization threshold needed for terminal UPR outputs (Ghosh, Wang et al. 2014). We treated T-Rex293 IRE1α (I642G) for 48hrs with Dox to induce the kinase-mutated inactive IRE1α (I642G) in the presence or absence of 1NMPP-1. Neither of these parameters affected AKT Ser473 phosphorylation after insulin stimulation **(Fig. 2.5B)**, indicating that XBP1s is not sufficient to inhibit the phosphorylation of AKT at Ser473 and that only the fully active form of IRE1α is able to affect AKT Ser473 phosphorylation. Moreover, results obtained with IRE1α (I642G) were indistinguishable from those in which the kinase-dead mutant of IRE1α (K599A), whose catalytic activities cannot be revived even in the presence 1NM-PP1, was used **(Fig. S2.3B)**. Therefore, these data suggest

that (1) the effects of IRE1α on AKT phosphorylation may not be through XBP1 and (2) IRE1α dependent terminal-UPR events are required for disruption of the insulin receptor signaling pathway. In order to test whether the kinase activity of IRE1α has any effect on AKT Ser473 phosphorylation, we used the kinase-active/RNase-mutant IRE1α (K907A). This mutant retains full phosphotransfer activity when expressed, but it does not splice XBP1 due to the mutation in its RNase active site **(Fig. S2.3C)** (Han, Lerner et al. 2009). As expected, overexpression of IRE1α (K907A) upon Dox treatment did not affect insulin-stimulated AKT Ser473 phosphorylation **(Fig. 2.5C)**. Altogether, these data suggest that IRE1α's catalytic activities are required to disrupt the insulin receptor signaling pathway through inhibition of AKT Ser473 phosphorylation.

Finally, we tested the effects of KIRA8 on glucose uptake in cells that experience ER stress when IRE1α is overexpressed. AKT Ser473 phosphorylation is crucial in the translocation of GLUT4 from the cytosol to the plasma membrane in order to enable glucose uptake. Given that KIRA8 rescues AKT Ser473 phosphorylation when IRE1α is overexpressed, we reasoned that cells should be able to absorb glucose when subjected to KIRA8 treatment under conditions that induce ER stress and subsequent IRE1α activation. To this end, we monitored glucose uptake in T-Rex293 cells overexpressing IRE1α using the fluorescent glucose analog 2-NBDG in the presence of KIRA8. Indeed, IRE1α overexpression prevented the cells from undergoing glucose uptake when treated with Dox for 48 hours, but KIRA8 increased glucose uptake as is indicated by the shift in the curve of Figure 2.5D **(Fig. 2.5D)**. The increase in glucose uptake supports the hypothesis that inhibition of IRE1α with KIRA8 improves systemic insulin signaling.

DISCUSSION

The results of this study have identified a previously unrecognized role of IRE1α in the development of insulin resistance through the disruption of the insulin receptor signaling pathway. Specifically, this study has provided both *ex vivo* and *in vivo* evidence showing that pharmacological inhibition of IRE1α with KIRA8 can potentiate the hepatic actions of insulin by enhancing glucose absorption through AKT activation. Moreover, administration of KIRA8 enhanced insulin responsiveness in the adipose tissue. Our studies show both the efficacious properties of KIRA8 to inhibit IRE1α and suppress UPR markers, and the versatility of KIRA8 to alleviate insulin resistance in more than one T2D mouse model. These findings also demonstrate a direct convergence of the UPR and the insulin receptor signaling pathways and suggest much cross-talk between these pathways.

Using chemical genetic tools, we also found that IRE1α hyperactivation is necessary and sufficient to blunt AKT Ser473 phosphorylation and decrease glucose uptake. In fact, overexpression of WT IRE1α blunted AKT Ser473 phosphorylation and suppressed glucose uptake through induction of 'T'-UPR outputs. Importantly, effects of IRE1α on AKT Ser473 phosphorylation may not occur through the adaptive outputs (i.e. XBP1 splicing) of IRE1α. To our knowledge, the involvement of the 'T'-UPR outputs of IRE1α in the disruption of the insulin receptor signaling pathway have not been described before; thus, our findings are entirely novel.

Even though we provide evidence that 'T'-UPR is necessary to suppress AKT Ser473 phosphorylation, the exact mechanism and players involved in this pathway remain to be elucidated. However, we propose that one of the key players involved in this

signaling pathway is the pro-apoptotic protein JNK. We were able to demonstrate in chapter 1 that the livers of vehicle-treated animals exhibited elevated levels of phosphorylation of c-Jun, a direct downstream target of JNK, and KIRA8 prevented c-Jun phosphorylation. Furthermore, c-Jun has been described as an essential player in the disruption of the insulin receptor signaling pathway (Ozcan, Cao et al. 2004). Previous work from our lab has shown that JNK is activated in an IRE1α-dependent manner and is a hallmark of the 'T'-UPR (Han, Lerner et al. 2009, Ghosh, Wang et al. 2014). In this chapter we were able to reproduce these results and correlate hyperactivation of IRE1α and phosphorylation of JNK with the reduced phosphorylation of AKT Ser473 **(Fig. 2.5A)**. Therefore, we hypothesize that IRE1α hyperactivation leads to the downstream phosphorylation of JNK, which leads to activation of c-Jun and disruption of the insulin receptor signaling pathway through the inhibition of AKT Ser473 phosphorylation. Still, future studies must be performed in order to further explore this potential mechanism.

The set of experiments performed in this investigation have led to the bridging of conceptual gaps and the elucidation of underlying mechanisms that will help us to better understand how to correct UPR-induced insulin resistance in physiologically relevant T2D murine models. Future studies will be needed to determine the precise mechanism by which IRE1α hyperactivation disrupts the insulin receptor signaling pathway through suppression of AKT Ser473 phosphorylation. These studies provide valuable insight into how targeting the IRE1α axis of the UPR with KIRA8 can restore faulty insulin signaling under ER stress, increase insulin sensitivity, and prevent or reverse T2D.

MATERIALS AND METHODS

Tissue Culture

HepG2 cells (human hepatocyte cell line), H4IIEC3 cells (rat hepatocyte cell line), and HEK293 T-REx cells (human embryonic kidney cell line) were grown and maintained in Dulbecco's Modified Eagle Media (DMEM) containing 5mM glucose. The DMEM was supplemented with 10% heat-inactivated fetal bovine serum (FBS, J.R. Scientific), 100U penicillin, and 100U streptomycin. Specifically, 1 mM sodium pyruvate and 10 mM HEPES was added to DMEM to grow the H4IIEC3 cells. For starvation, cells were maintained in FBS-free media for the indicated times in their respective experiments.

Western Blots and Antibodies

For protein analysis, cells were lysed in M-PER buffer (Thermo Scientific) or T-PER buffer for ~100 mg of mouse tissue plus complete EDTA-free protease inhibitor and phosphatase inhibitor (Roche). Protein concentration was determined using Rapid Gold BCA Protein Assay (Thermo). Western blots were performed using 4%–12% Bis-Tris (NuPage). Gels were migrated using MES buffer and transferred onto nitrocellulose transfer membrane using an iBlot 2 Dry Blotting System (Themro). Antibody binding was detected with near-infrared- dye-conjugated secondary antibodies (Li-Cor) on the LI-COR Odyssey scanner. Blocking, antibody incubation, and washing were done in TBS with 0.05% Tween-20 (v/v). Antibody-binding was detected with near-infrared- dye-conjugated secondary antibodies (Li-Cor) on the LI-COR Odyssey scanner and quantified by

densitometry using ImageJ (NIH). GAPDH and Actin were used as a loading control. For a list of antibodies and the dilutions used, please see Table 2.1.

RNA Isolation, Quantitative Real-time PCR, and Primers

RNA was isolated from tissue using Trizol (Invitrogen). For standard mRNA detection, generally 1 μg total RNA was reverse transcribed using the QuantiTect Reverse Transcription Kit (QIAGEN). For qPCR, we used SYBR green (QIAGEN) and StepOnePlus Real-Time PCR System (Applied Biosystems). Thermal cycles were: 5 min at 95°C, 40 cycles of 15 s at 95°C, 30 s at 60°C. Gene expression levels were normalized to 18S rRNA. Primers used for qPCR can be found in Table 2.2.

XBP1 mRNA Splicing

RNA was isolated from tissues and reverse transcribed as above to obtain total cDNA. Then, XBP1 primers were used to amplify an XBP-1 amplicon spanning the 26 nt intron from the cDNA samples in a regular 3-step PCR. Thermal cycles were: 5 min at 95°C, 30 cycles of 30 sec at 95°C, 30 sec at 60°C, and 1 min at 72°C, followed by 72°C for 15 min, and hold at 4°C. Primers used for XBP1 mRNA splicing were as follows: human sense primer (5′- GTATCTCTAAGACTAGGGGCTTGG -3′), human antisense primer (5′- AAACAGAGTAGCAGCTCAGACTGC -3′), rat sense primer (5′- AGGAAACTGAAAAACAGAGTAGCAGC-3′), and rat antisense primer (5′- TCCTTCTGGGTAGACCTCTGG -3′). PCR fragments were then digested by PstI, resolved on 3% agarose gels, stained with EtBr and quantified by densitometry using ImageJ (NIH).

AKT Ser473 determination assay

HepG2 and H4IIEC3 cells were pretreated with KIRA8 for 1 hour before starting treatment with ER stress agents. Later, Tunicamycin (EMD Millipore), Brefeldin A (Sigma), or Palmitate (Nu-Check Prep) was added to the media and cells were incubated at 37°C in FBS-free media. After 24 hours, insulin at the specified concentration was added to the media and cells were incubated for 5 minutes. AKT Ser 473 phosphorylation was then analyzed by western blot. For T-Rex293 cells, they were pretreated with KIRA8 for 1 hour before administration of Dox. Cells were then co-treated with KIRA8 and Dox (1 μg/mL) for 48 hours, incubated for the last 24 hours in FBS-free media. After 48 hours, AKT Ser473 phosphorylation was stimulated upon addition of 10 nM of insulin for 5 minutes and determined through western blot.

Glucose (2-NBD) uptake experiment in T-Rex293 cells

For assaying glucose uptake, cells were plated in 10 cm dishes overnight. Same conditions as for determination of AKT Ser473 phosphorylation were used but cells where incubated for the last 24 hours in FBS- and glucose-free media. Insulin (10 nM) and 2-NBDG (150 μg/mL) was then added and cells were incubated for 1 hour at 37°C. On the day of analysis, cells were trypsinized and washed in PBS and resuspended in provided buffer (Cayman, Ann Arbor, MI). Flow cytometry was performed on a Becton Dickinson LSRII flow cytometer.

Statistical Analysis

All statistical analyses were performed using GraphPad Prism version 8.1. Student's t test or one-way ANOVA were applied to determine statistical difference between two groups. Data are presented as mean ± SEM $p < 0.05$ was considered significant throughout the study. p values: * < 0.05; ** < 0.01; *** < 0.001; N.S., non-significant

TABLE 2.1. List of antibodies used for western blot

Antibody	Source (Catalog number)	Dilution
p-c-Jun	CST (# 9164)	1:1000
total c-Jun	CST (# 9165)	1:1000
XBP1	Proteintech (# 25997-1-AP)	1:1000
BiP	CST (# 3177)	1:1000
p-IRE1α Ser724	Novus Biologicals (# NB100-2323)	1:500
total IRE1α	CST (# 3294)	1:1000
Myc	Santa Cruz Biotechnology (# sc-40)	1:1000
p-AKT Ser473	CST (# 9271)	1:1000
total AKT	CST (# 9272)	1:1000
Actin	Santa Cruz Biotechnology (# sc-47778)	1:2000
GAPDH	CST (# 2118)	1:2000

TABLE 2.2. List of primers used for qPCR to determine UPR markers in mouse livers

Gene	Forward Primer	Reverse Primer
ATF4	GCAAGGAGGATGCCTTTTC	GTTTCCAGGTCATCCATTCG
XBP1	CCGTGAGTTTTCTCCCGTAA	AGAAAGAAAGCCCGGATGAG
CHOP	CTCCAGATTCCAGTCAGAGTTC	CCACTCTGTTTCCGTTTCCTA
BIP	GCATATGGCCTGGATAAGAGAG	GTCAATGGTGAGAAGAGACACA
18s	GTAACCCGTTGAACCCCATT	CCATCCAATCGGTAGTAGGC

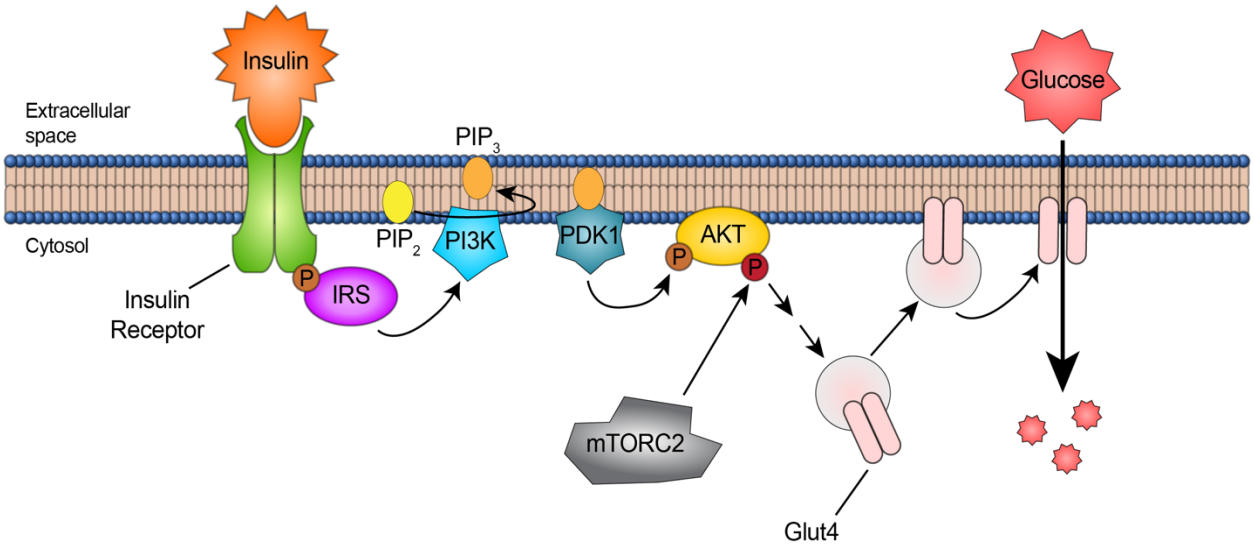

Figure 2.1. Diagram of the insulin receptor signaling pathway.

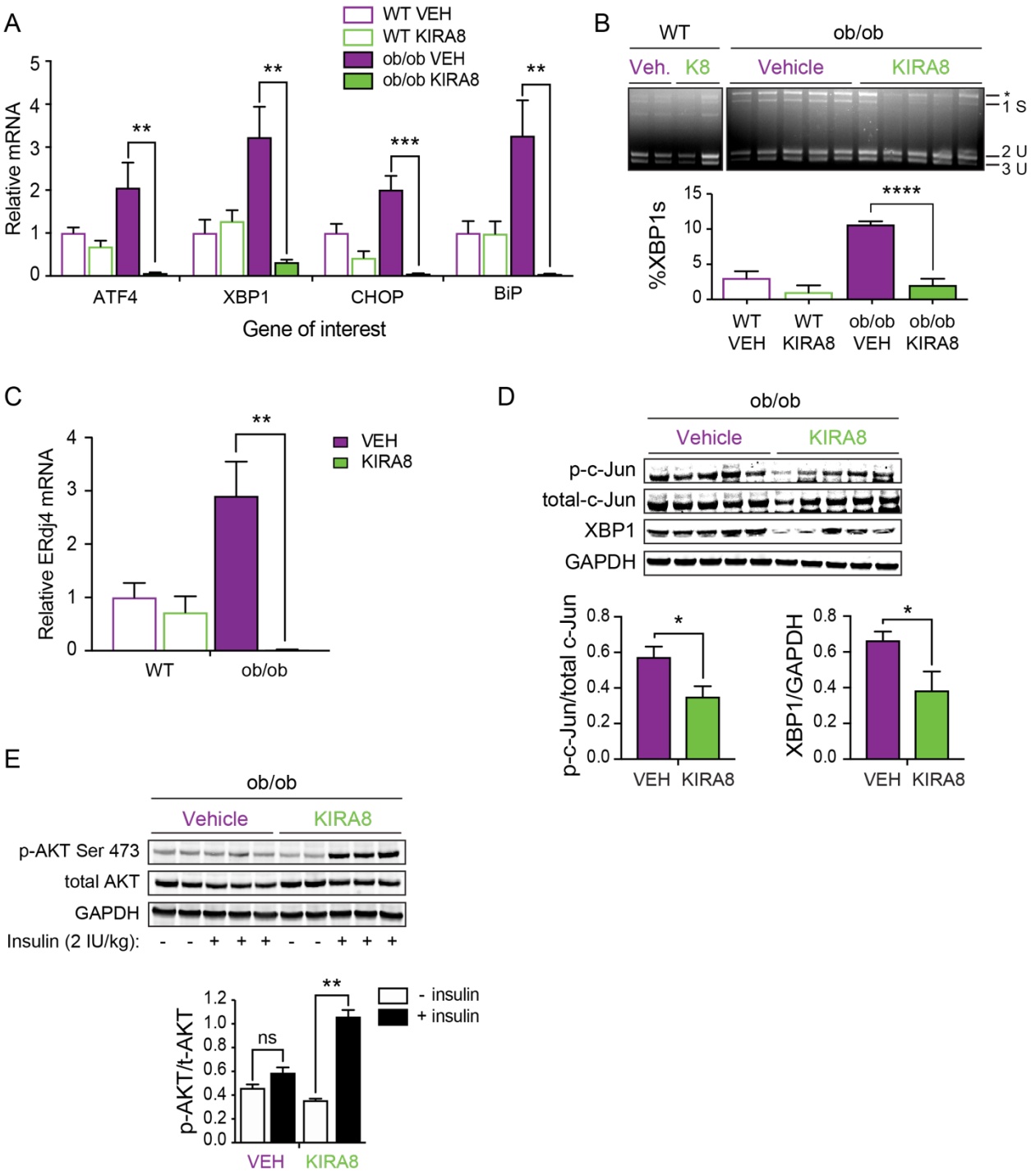

Figure 2.2. KIRA8 reduces obesity-induced ER stress markers in the liver of BTBR*lep*$^{ob/ob}$ mice and restores AKT Ser473 phosphorylation.
(A) Relative mRNAs levels in liver tissue from WT BTBR and BTBR*lep*$^{ob/ob}$ mice treated with KIRA8 (50 mg/kg) or vehicle for 28 days. Bars represent means ± SEM. p values: * < 0.05, ** < 0.01, *** < 0.001.

(B) Agarose gel of PstI-digested XBP1 cDNA amplicons from liver tissue of 4 weeks KIRA8- or vehicle-treated WT BTBR and BTBR*lep*$^{ob/ob}$ mice. Each lane is from an individual mouse. Graph represents ratiometric quantitation of spliced to total XBP1 cDNA. Bars represent means ± SEM. p values: * < 0.05, ** < 0.01, *** < 0.001.
(C) Immunoblots for ER stress markers c-Jun (Ser-73) phosphorylation and XBP1s in liver tissues of 4 weeks KIRA8- and vehicle-treated BTBR*lep*$^{ob/ob}$ mice. Each lane is from an individual mouse. Graphs represent signal intensity ratios. Bars represent means ± SEM. p values: * < 0.05.
(D) Immunoblots for AKT Ser473 phosphorylation and total AKT in liver tissues of 4 weeks KIRA8- and vehicle-treated BTBR*lep*$^{ob/ob}$ mice. For this specific experiment, mice were fasted for 18 hrs and then stimulated with an intraperitoneal injection of insulin (2 IU/kg). Each lane is from an individual mouse. Graphs represent signal intensity ratios. Bars represent means ± SEM. p values: * < 0.05, ** < 0.01.

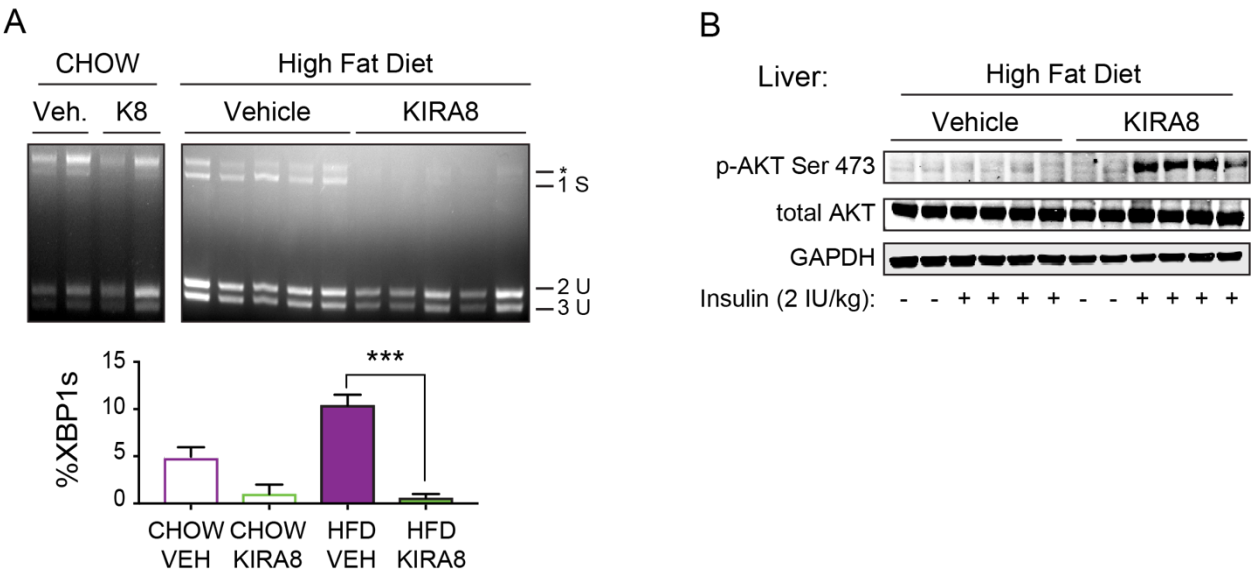

Figure 2.3. KIRA8 reduces XBP1 splicing in the liver of HFD fed-mice and restores AKT Ser473 phosphorylation.

(A) Agarose gel of PstI-digested XBP1 cDNA amplicons from liver of C57BL/6J mice fed with either regular CHOW or HFD and treated with vehicle or KIRA8 for 28 days. Each lane is from an individual mouse. Graph represents ratiometric quantitation of spliced to total XBP1 cDNA. Bars represent means ± SEM. p values: * < 0.05, ** < 0.01, *** < 0.001.

(B) Immunoblots for AKT Ser473 phosphorylation and total AKT in the liver. Mice were fasted for 6 hrs and stimulated then stimulated with insulin (1IU/kg) for 20 mins. Each lane is from an individual mouse. Graphs represent signal intensity ratios. Bars represent means ± SEM. p values: * < 0.05, ** < 0.01.

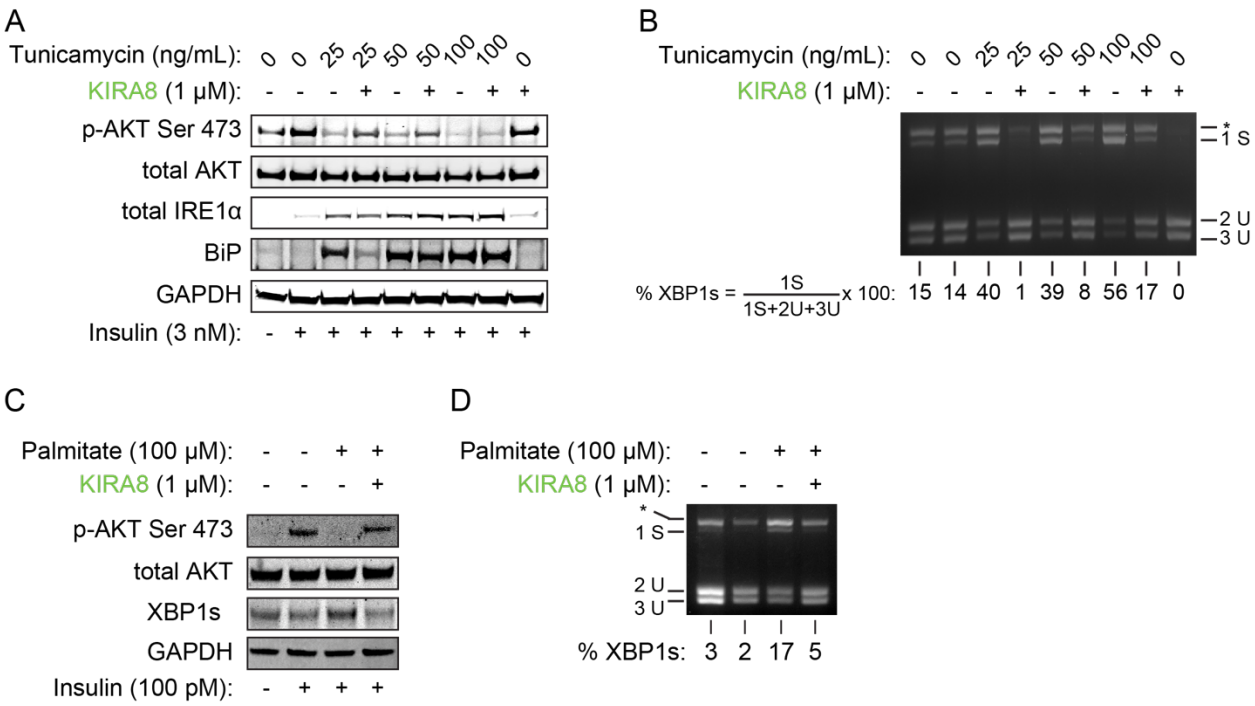

Figure 2.4. Chemically-induced ER stress blunts AKT phosphorylation and KIRA8 rescues it in HepG2 and H4IIEC3 cells.
(A) ER stress was induced in HepG2 liver cells by a 24-hour treatment with tunicamycin at different concentrations in the presence or absence of KIRA8 (1 μM). Cells were subsequently stimulated with insulin (3 nM) for 10 minutes. AKT Ser473 phosphorylation and its total protein levels, total IRE1α, and BiP were examined by direct immunoblotting.
(B) Agarose gel of PstI-digested XBP1 cDNA amplicons (ratiometric quantitation of spliced to total XBP1 cDNAs) from (A).
(C and D) AKT Ser473 phosphorylation (C) and XBP1 splicing (D) in H4IIEC3 cells subjected to Palmitate in the absence or presence of KIRA8 for 24 hours in FBS-free media followed by an insulin stimulation for 5 minutes.

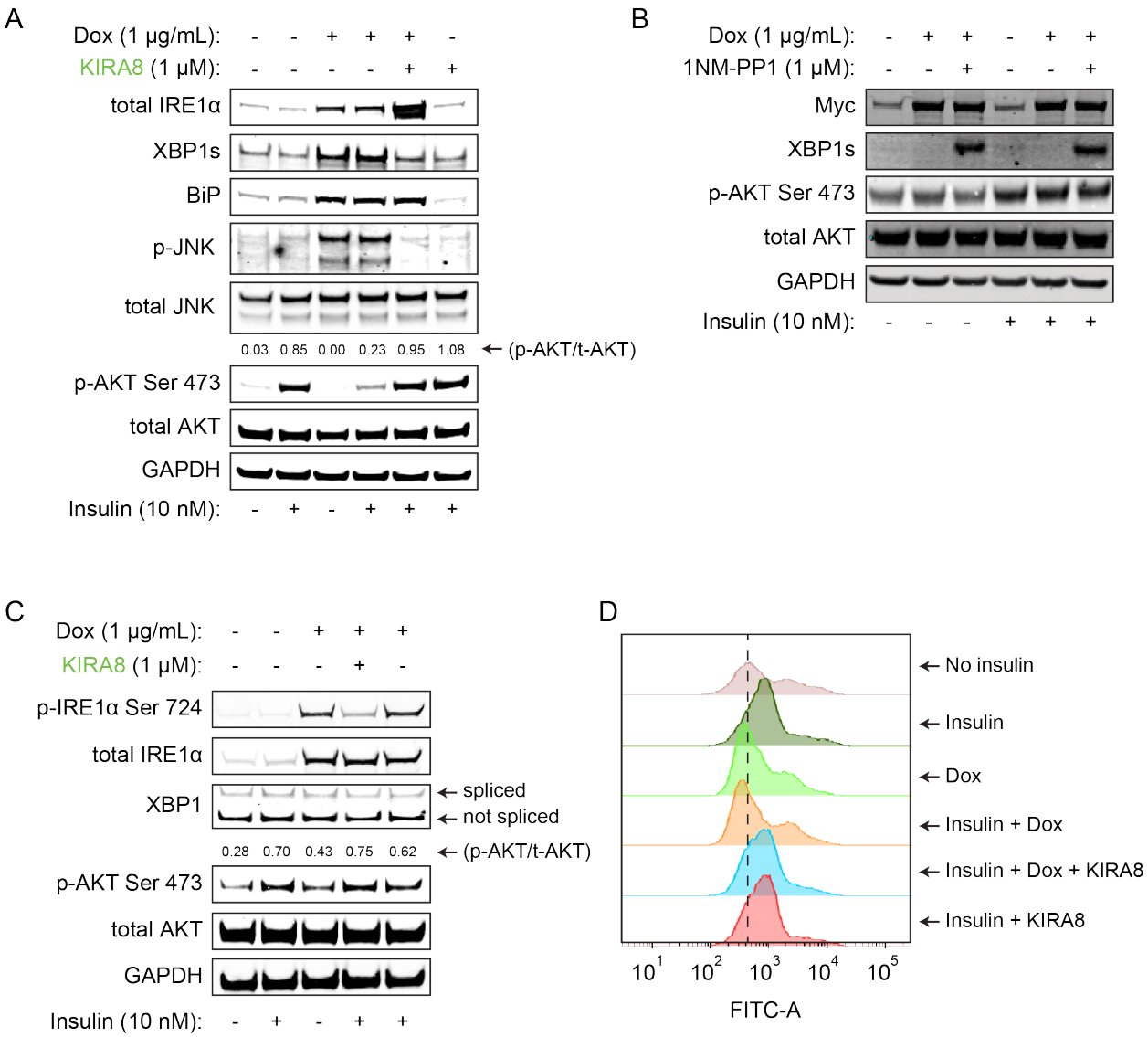

Figure 2.5. IRE1α 'T'-UPR outputs are necessary and sufficient to blunt AKT Ser473 phosphorylation and reduce glucose uptake *in vitro*.
(A) Immunoblots for total IRE1α, XBP1s, BiP, p-JNK, total JNK, and AKT Ser473 phosphorylation in T-Rex-293 cells overexpressing transgenic WT IRE1α upon doxycycline treatment for 48 hours in the presence or absence of KIRA8. Cells were FBS-deprived for the last 24 hours of the experiment and then insulin stimulated for 5 minutes. **(B and C)** Immunoblot analysis of Myc-tagged total IRE1α and AKT Ser473 phosphorylation in T-Rex293 cells overexpressing IRE1α mutants I642G (B) and K907A (C) using the same conditions as in (A). XBP1s was forcibly expressed in (B) upon addition of 1 μM 1NM-PP1 to the cells.
(D) Glucose uptake in T-Rex-293 cells overexpressing WT IRE1α in the presence of KIRA8. Cells were incubated with insulin (10 nM) and the fluorescent glucose analog 2-NBDG (150 μg/mL) for 1 hour after 48 hours of Dox treatment.

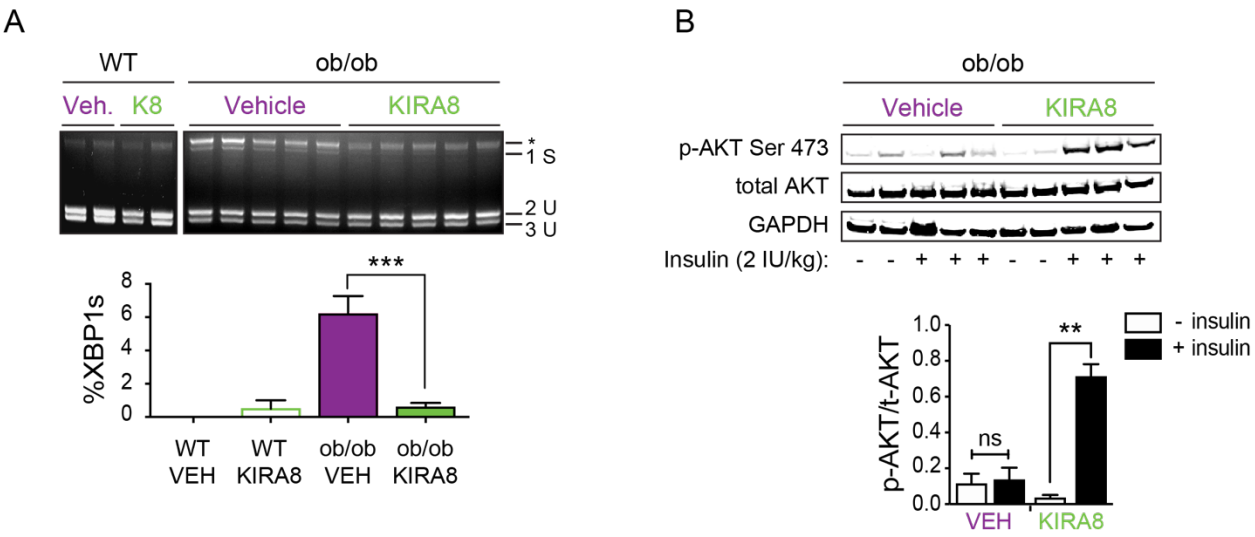

Figure S2.1. KIRA8 reduces obesity-induced XBP1 splicing in the adipose tissue of BTBR*lep*$^{ob/ob}$ mice and restores AKT Ser473 phosphorylation.
(A) Agarose gel of PstI-digested XBP1 cDNA amplicons from adipose tissue of 4 weeks KIRA8- or vehicle-treated WT BTBR and BTBR*lep*$^{ob/ob}$ mice. Each lane is from an individual mouse. Graph represents ratiometric quantitation of spliced to total XBP1 cDNA. Bars represent means ± SEM. p values: * < 0.05, ** < 0.01, *** < 0.001.
(B) Immunoblots for AKT Ser473 phosphorylation and total AKT in adipose tissues of 4 weeks KIRA8- and vehicle-treated BTBR*lep*$^{ob/ob}$ mice. For this specific experiment, mice were fasted for 18 hrs and then stimulated with an intraperitoneal injection of insulin (2 IU/kg). Each lane is from an individual mouse. Graphs represent signal intensity ratios. Bars represent means ± SEM. p values: * < 0.05, ** < 0.01.

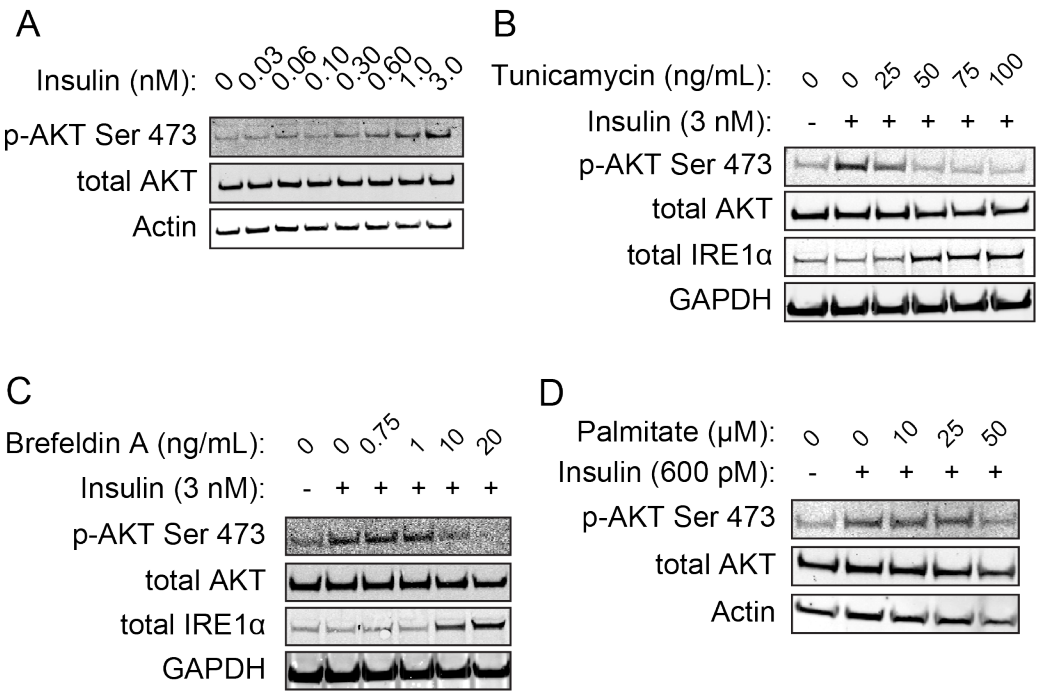

Figure S2.2. Different chemical ER stress inducers blunt AKT Ser473 phosphorylation in HepG2 hepatocytes.
(A) Insulin-stimulated AKT Ser473 phosphorylation in HepG2 cells after 24 hours incubation in FBS-free media using different insulin concentrations for 10 minutes.
(B - D) Different concentrations of Tunicamycin (B), Brefeldin A (C), and Palmitate (D) blunt AKT Ser473 phosphorylation and upregulates IRE1α. HepG2 cells were insulin stimulated for 10 minutes after a 24 hours treatment of each chemical ER stress-agent in FBS-free media.

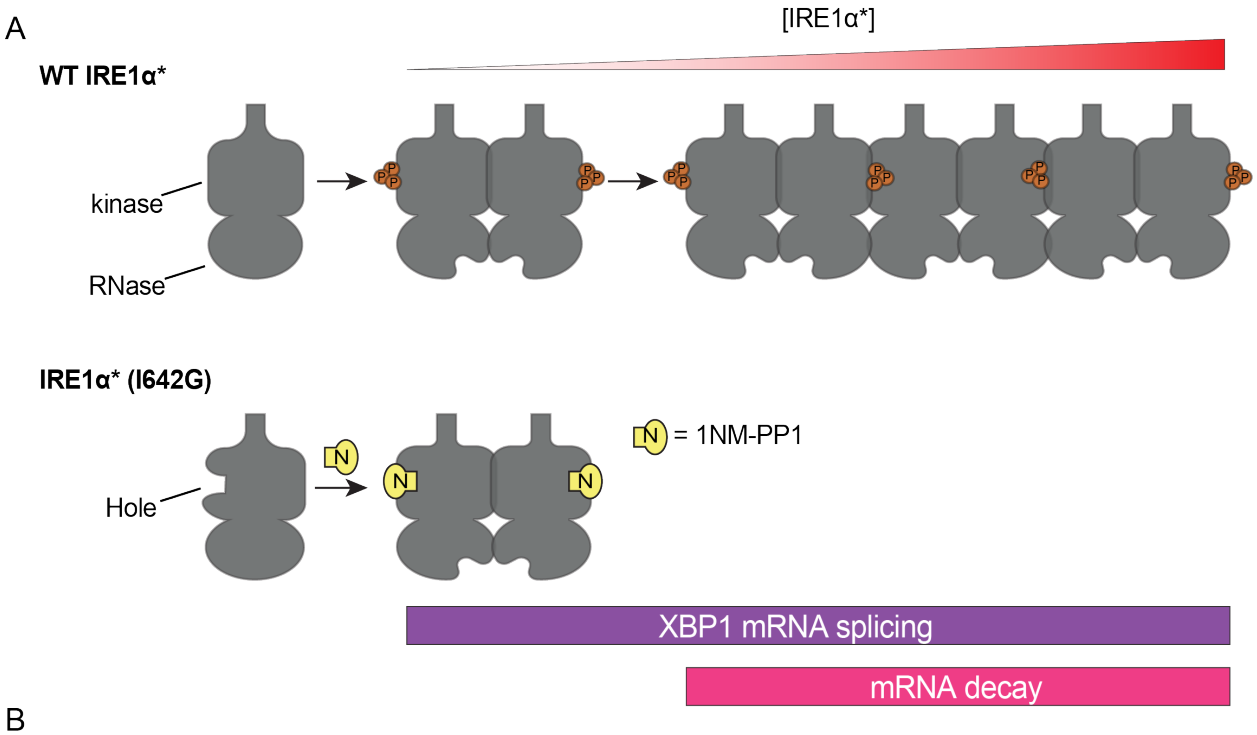
A
[IRE1α*]
WT IRE1α*
kinase
RNase
IRE1α* (I642G)
Hole
N
= 1NM-PP1
XBP1 mRNA splicing
mRNA decay

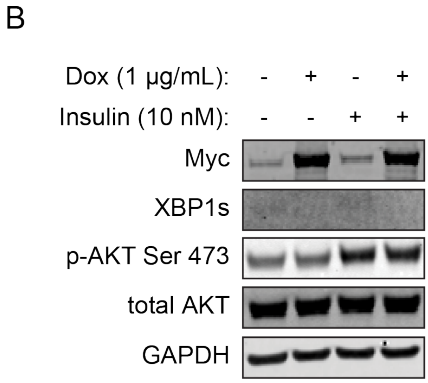
B
Dox (1 μg/mL): - + - +
Insulin (10 nM): - - + +
Myc
XBP1s
p-AKT Ser 473
total AKT
GAPDH

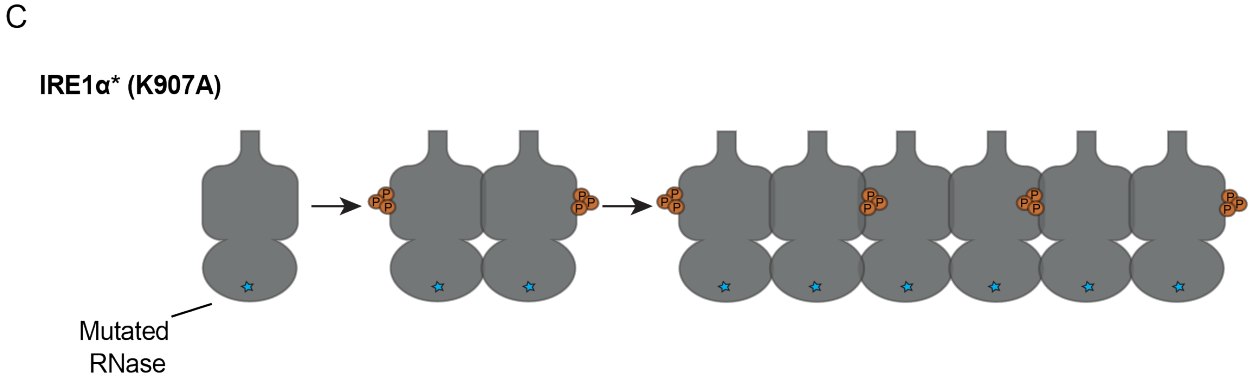
C
IRE1α* (K907A)
Mutated
RNase

Figure S2.3. Conditional Tools to Forcibly Trigger IRE1α Catalytic Activities.
(A) Diagram showing the differences in levels of activation and different outputs achieved by transgenic WT IRE1α* and IRE1α* (I642G).
(B) Immunoblot analysis of Myc-tagged total IRE1α and AKT Ser473 phosphorylation in T-Rex293 expressing the IRE1α kinase-dead mutant K599A, using the same conditions as in Figure 2.5B.
(C) RNase-dead IRE1α* (K907A) mutant used in this study.

CHAPTER 3

Conclusions and Future Directions

CONCLUSIONS

We found that IRE1α is sufficient to disrupt the insulin receptor signaling pathway. Specifically, the terminal UPR outputs of IRE1α are required to desensitize cells *in vitro* and *in vivo* to insulin. IRE1α can promote homeostasis through the unconventional splicing of XBP1, which is a very potent transcription factor that promotes adaptation to ER stress. Administration of KIRA8 *in vivo* in Chapter 1 demonstrated that XBP1 is barely spliced in liver and adipose tissue and correlates with the rescue in AKT Ser473 phosphorylation. However, using our *in vitro* genetic tools in Chapter 2 to distinguish between the adaptive and terminal outputs of IRE1α, we found that the rescue of AKT phosphorylation at Ser473 may not occur through the splicing of XBP1, as HEK cells overexpressing the mutant versions of IRE1α I642G and K907A, did not undergo changes in AKT Ser473 phosphorylation. Altogether, our *in vitro* and *in vivo* data suggest (1) that IRE1α's adaptive outputs (i.e. XBP1 splicing) might be overshadowed by its terminal outputs in the context of insulin resistance and (2) IRE1α hyperactivation and subsequent destructive outputs are essential in the development and progression of insulin resistance. The mechanism by which these IRE1α-destructive outputs blunt AKT Ser473 phosphorylation remains unknown but will be addressed in future experiments.

Our findings also show the efficacious properties of KIRA8 as an inhibitor of IRE1α in different mouse models of insulin resistance. Not only we were able to ameliorate insulin resistance and prevent hyperglycemia, but we also provide evidence of the positive physiological effects that KIRA8 provides *in vivo*. For instance, KIRA8 improved triglycerides and ketones levels, and reduced the formation of fat in the livers of mice. An unexpected side effect was the reduction in the rate at which KIRA8-treated animals

gained weight. More studies are necessary to determine if KIRA8 can control body weight or if these effects are due to systemic effects on other tissues that are known to control appetite (i.e. hypothalamus).

Finally, this dissertation has contributed to our current understanding of insulin resistance development in the context of obesity-induced ER stress. We discovered that inhibition of IRE1α with a small molecule restores insulin sensitivity and responsiveness, and improves whole-body glucose homeostasis. More importantly, this investigation revealed the importance of IRE1α as key modulator in the progression of proteostasis diseases.

FUTURE DIRECTIONS

Even though it is known that AKT is a direct substrate of the mammalian Target of Rapamycin Complex 2 (mTORC2), our analyses did not reveal changes in phosphorylation or mRNA levels in any of the members of this complex during ER stress induction (data not shown). Therefore, future work should be aimed at addressing the specific mechanism by which 'T'-UPR outputs of IRE1α prevent the phosphorylation of AKT at Ser473. Here, we propose at least two different pathways that may contribute to the IRE1α-dependent disruption of the insulin receptor signaling pathway that warrant further investigation.

First, as mentioned above, it is important to continue exploring the exact role of JNK in preventing AKT Ser473 phosphorylation. Previous work has shown that ER stress impairs insulin action through JNK (Ozcan, Cao et al. 2004). On the other hand, we have demonstrated before that activation of JNK is an important component of the destructive

outputs of IRE1α (Ghosh, Wang et al. 2014). Therefore, it is reasonable to believe that JNK represents a point of convergence between IRE1α hyperactivation and the reduction in AKT Ser473 phosphorylation. We have shown data to support the notion that phosphorylation of c-Jun (a direct target of JNK) is reduced in diabetic animals treated with KIRA8, which correlates with an increase phosphorylation of AKT at Ser473. Moreover, KIRA8 was able to prevent JNK phosphorylation while rescuing AKT Ser473 phosphorylation in an *in vitro* system where IRE1α is upregulated and its catalytic activities were forcibly activated without upstream ER stress. Nonetheless, more experiments need to be performed to determine the requirement of JNK in this context.

The second molecular mechanism that we propose involves the participation of the protein TRB3, a mammalian homolog of Drosophila tribbles. TRB3 has previously been described as a negative modulator of AKT. Specifically, it has been shown that TRB3, which expression is induced in the liver under fasting conditions, interacts directly with AKT and prevents its phosphorylation at Ser473 in the liver of diabetic mice (Du, Herzig et al. 2003). In turn, this leads to hyperglycemia, glucose intolerance and a reduction in insulin responsiveness. Encouraged by these observations, we looked at the expression of hepatic TRB3 in the BTBR*lep*$^{ob/ob}$ mice treated with vehicle or KIRA8. Interestingly, TRB3 is upregulated in the vehicle-treated BTBR*lep*$^{ob/ob}$ mice in comparison to mice treated with KIRA8 (data not shown). Therefore, we believe that this other signaling pathway warrants further investigation as TRB3 is known to be controlled by microRNAs and we have shown that, under chronic ER stress, IRE1α cleaves many ER-localized microRNAs (Chan, Hilyard et al. 2010, Upton, Wang et al. 2012, Liu, Zhao et al. 2016). It is possible that, when hyperactivated, IRE1α degrades TRB3 one of the

microRNAs that regulate the expression of this protein, leading to upregulation of TRB3 and subsequent disruption of the insulin receptor signaling pathway via the TRB3-AKT direct interaction. More studies are required to confirm this proposed mechanism.

Finally, the *in vivo* work that we present here is solely based on a high fat diet and obesity-induced insulin resistance. However, there are other major risk factors that contribute to the development of insulin resistance and T2D, including a familial history of diabetes and lack of exercise. Therefore, it still remains to be investigated if the efficacious properties of KIRA8 to ameliorate insulin resistance and prevent the development of T2D can be maintained in the context of these other risk factors.

REFERENCES

Acosta-Alvear, D., Y. Zhou, A. Blais, M. Tsikitis, N. H. Lents, C. Arias, C. J. Lennon, Y. Kluger and B. D. Dynlacht (2007). "XBP1 controls diverse cell type- and condition-specific transcriptional regulatory networks." Mol Cell **27**(1): 53-66.

Adachi, Y., K. Yamamoto, T. Okada, H. Yoshida, A. Harada and K. Mori (2008). "ATF6 is a transcription factor specializing in the regulation of quality control proteins in the endoplasmic reticulum." Cell Struct Funct **33**(1): 75-89.

Alessi, D. R., F. B. Caudwell, M. Andjelkovic, B. A. Hemmings and P. Cohen (1996). "Molecular basis for the substrate specificity of protein kinase B; comparison with MAPKAP kinase-1 and p70 S6 kinase." FEBS Lett **399**(3): 333-338.

Balsa, E., M. S. Soustek, A. Thomas, S. Cogliati, C. Garcia-Poyatos, E. Martin-Garcia, M. Jedrychowski, S. P. Gygi, J. A. Enriquez and P. Puigserver (2019). "ER and Nutrient Stress Promote Assembly of Respiratory Chain Supercomplexes through the PERK-eIF2alpha Axis." Mol Cell **74**(5): 877-890 e876.

Bays, H. E., R. H. Chapman, S. Grandy and S. I. Group (2007). "The relationship of body mass index to diabetes mellitus, hypertension and dyslipidaemia: comparison of data from two national surveys." Int J Clin Pract **61**(5): 737-747.

Bobrovnikova-Marjon, E., C. Grigoriadou, D. Pytel, F. Zhang, J. Ye, C. Koumenis, D. Cavener and J. A. Diehl (2010). "PERK promotes cancer cell proliferation and tumor growth by limiting oxidative DNA damage." Oncogene **29**(27): 3881-3895.

Bommiasamy, H., S. H. Back, P. Fagone, K. Lee, S. Meshinchi, E. Vink, R. Sriburi, M. Frank, S. Jackowski, R. J. Kaufman and J. W. Brewer (2009). "ATF6alpha induces XBP1-independent expansion of the endoplasmic reticulum." J Cell Sci **122**(Pt 10): 1626-1636.

Butler, A. E., J. Janson, S. Bonner-Weir, R. Ritzel, R. A. Rizza and P. C. Butler (2003). "Beta-cell deficit and increased beta-cell apoptosis in humans with type 2 diabetes." Diabetes **52**(1): 102-110.

Calfon, M., H. Zeng, F. Urano, J. H. Till, S. R. Hubbard, H. P. Harding, S. G. Clark and D. Ron (2002). "IRE1 couples endoplasmic reticulum load to secretory capacity by processing the XBP-1 mRNA." Nature **415**(6867): 92-96.

Chan, M. C., A. C. Hilyard, C. Wu, B. N. Davis, N. S. Hill, A. Lal, J. Lieberman, G. Lagna and A. Hata (2010). "Molecular basis for antagonism between PDGF and the TGFbeta family of signalling pathways by control of miR-24 expression." EMBO J **29**(3): 559-573.

Chen, J., S. T. Hui, F. M. Couto, I. N. Mungrue, D. B. Davis, A. D. Attie, A. J. Lusis, R. A. Davis and A. Shalev (2008). "Thioredoxin-interacting protein deficiency induces Akt/Bcl-xL signaling and pancreatic beta-cell mass and protects against diabetes." FASEB J **22**(10): 3581-3594.

Cnop, M., F. Foufelle and L. A. Velloso (2012). "Endoplasmic reticulum stress, obesity and diabetes." Trends Mol Med **18**(1): 59-68.

Del Guerra, S., R. Lupi, L. Marselli, M. Masini, M. Bugliani, S. Sbrana, S. Torri, M. Pollera, U. Boggi, F. Mosca, S. Del Prato and P. Marchetti (2005). "Functional and molecular defects of pancreatic islets in human type 2 diabetes." Diabetes **54**(3): 727-735.

Du, K., S. Herzig, R. N. Kulkarni and M. Montminy (2003). "TRB3: a tribbles homolog that inhibits Akt/PKB activation by insulin in liver." Science **300**(5625): 1574-1577.

Flamment, M., E. Hajduch, P. Ferre and F. Foufelle (2012). "New insights into ER stress-induced insulin resistance." Trends Endocrinol Metab **23**(8): 381-390.

Fu, Z., E. R. Gilbert and D. Liu (2013). "Regulation of insulin synthesis and secretion and pancreatic Beta-cell dysfunction in diabetes." Curr Diabetes Rev **9**(1): 25-53.

Gething, M. J. and J. Sambrook (1990). "Transport and assembly processes in the endoplasmic reticulum." Semin Cell Biol **1**(1): 65-72.

Ghosh, R., L. Wang, E. S. Wang, B. G. Perera, A. Igbaria, S. Morita, K. Prado, M. Thamsen, D. Caswell, H. Macias, K. F. Weiberth, M. J. Gliedt, M. V. Alavi, S. B. Hari, A. K. Mitra, B. Bhhatarai, S. C. Schurer, E. L. Snapp, D. B. Gould, M. S. German, B. J. Backes, D. J. Maly, S. A. Oakes and F. R. Papa (2014). "Allosteric inhibition of the

IRE1alpha RNase preserves cell viability and function during endoplasmic reticulum stress." Cell **158**(3): 534-548.

Grote, C. W., A. L. Groover, J. M. Ryals, P. C. Geiger, E. L. Feldman and D. E. Wright (2013). "Peripheral nervous system insulin resistance in ob/ob mice." Acta Neuropathol Commun **1**: 15.

Han, D., A. G. Lerner, L. Vande Walle, J. P. Upton, W. Xu, A. Hagen, B. J. Backes, S. A. Oakes and F. R. Papa (2009). "IRE1alpha kinase activation modes control alternate endoribonuclease outputs to determine divergent cell fates." Cell **138**(3): 562-575.

Harding, H. P., I. Novoa, Y. Zhang, H. Zeng, R. Wek, M. Schapira and D. Ron (2000). "Regulated translation initiation controls stress-induced gene expression in mammalian cells." Mol Cell **6**(5): 1099-1108.

Harding, H. P., Y. Zhang, A. Bertolotti, H. Zeng and D. Ron (2000). "Perk is essential for translational regulation and cell survival during the unfolded protein response." Mol Cell **5**(5): 897-904.

Harding, H. P., Y. Zhang and D. Ron (1999). "Protein translation and folding are coupled by an endoplasmic-reticulum-resident kinase." Nature **397**(6716): 271-274.

Harrington, P. E., K. Biswas, D. Malwitz, A. S. Tasker, C. Mohr, K. L. Andrews, K. Dellamaggiore, R. Kendall, H. Beckmann, P. Jaeckel, S. Materna-Reichelt, J. R. Allen

and J. R. Lipford (2015). "Unfolded Protein Response in Cancer: IRE1alpha Inhibition by Selective Kinase Ligands Does Not Impair Tumor Cell Viability." ACS Med Chem Lett **6**(1): 68-72.

Hatting, M., C. D. J. Tavares, K. Sharabi, A. K. Rines and P. Puigserver (2018). "Insulin regulation of gluconeogenesis." Ann N Y Acad Sci **1411**(1): 21-35.

Hetz, C., E. Chevet and H. P. Harding (2013). "Targeting the unfolded protein response in disease." Nat Rev Drug Discov **12**(9): 703-719.

Hollien, J., J. H. Lin, H. Li, N. Stevens, P. Walter and J. S. Weissman (2009). "Regulated Ire1-dependent decay of messenger RNAs in mammalian cells." J Cell Biol **186**(3): 323-331.

Hollien, J. and J. S. Weissman (2006). "Decay of endoplasmic reticulum-localized mRNAs during the unfolded protein response." Science **313**(5783): 104-107.

Hudkins, K. L., W. Pichaiwong, T. Wietecha, J. Kowalewska, M. C. Banas, M. W. Spencer, A. Muhlfeld, M. Koelling, J. W. Pippin, S. J. Shankland, B. Askari, M. E. Rabaglia, M. P. Keller, A. D. Attie and C. E. Alpers (2010). "BTBR Ob/Ob mutant mice model progressive diabetic nephropathy." J Am Soc Nephrol **21**(9): 1533-1542.

Imagawa, Y., A. Hosoda, S. Sasaka, A. Tsuru and K. Kohno (2008). "RNase domains determine the functional difference between IRE1alpha and IRE1beta." FEBS Lett **582**(5): 656-660.

Iwawaki, T., A. Hosoda, T. Okuda, Y. Kamigori, C. Nomura-Furuwatari, Y. Kimata, A. Tsuru and K. Kohno (2001). "Translational control by the ER transmembrane kinase/ribonuclease IRE1 under ER stress." Nat Cell Biol **3**(2): 158-164.

Kim, K. E., Y. Jung, S. Min, M. Nam, R. W. Heo, B. T. Jeon, D. H. Song, C. O. Yi, E. A. Jeong, H. Kim, J. Kim, S. Y. Jeong, W. Kwak, H. Ryu do, T. L. Horvath, G. S. Roh and G. S. Hwang (2016). "Caloric restriction of db/db mice reverts hepatic steatosis and body weight with divergent hepatic metabolism." Sci Rep **6**: 30111.

Klippel, A., W. M. Kavanaugh, D. Pot and L. T. Williams (1997). "A specific product of phosphatidylinositol 3-kinase directly activates the protein kinase Akt through its pleckstrin homology domain." Mol Cell Biol **17**(1): 338-344.

Koh, H. J., T. Toyoda, M. M. Didesch, M. Y. Lee, M. W. Sleeman, R. N. Kulkarni, N. Musi, M. F. Hirshman and L. J. Goodyear (2013). "Tribbles 3 mediates endoplasmic reticulum stress-induced insulin resistance in skeletal muscle." Nat Commun **4**: 1871.

Kokame, K., H. Kato and T. Miyata (2001). "Identification of ERSE-II, a new cis-acting element responsible for the ATF6-dependent mammalian unfolded protein response." J Biol Chem **276**(12): 9199-9205.

Lee, A. H., N. N. Iwakoshi and L. H. Glimcher (2003). "XBP-1 regulates a subset of endoplasmic reticulum resident chaperone genes in the unfolded protein response." Mol Cell Biol **23**(21): 7448-7459.

Lee, A. H., E. F. Scapa, D. E. Cohen and L. H. Glimcher (2008). "Regulation of hepatic lipogenesis by the transcription factor XBP1." Science **320**(5882): 1492-1496.

Lerner, A. G., J. P. Upton, P. V. Praveen, R. Ghosh, Y. Nakagawa, A. Igbaria, S. Shen, V. Nguyen, B. J. Backes, M. Heiman, N. Heintz, P. Greengard, S. Hui, Q. Tang, A. Trusina, S. A. Oakes and F. R. Papa (2012). "IRE1alpha induces thioredoxin-interacting protein to activate the NLRP3 inflammasome and promote programmed cell death under irremediable ER stress." Cell Metab **16**(2): 250-264.

Liu, X., J. Zhao, Q. Liu, X. Xiong, Z. Zhang, Y. Jiao, X. Li, B. Liu, Y. Li and Y. Lu (2016). "MicroRNA-124 promotes hepatic triglyceride accumulation through targeting tribbles homolog 3." Sci Rep **6**: 37170.

Mahameed, M., T. Wilhelm, O. Darawshi, A. Obiedat, W. S. Tommy, C. Chintha, T. Schubert, A. Samali, E. Chevet, L. A. Eriksson, M. Huber and B. Tirosh (2019). "The unfolded protein response modulators GSK2606414 and KIRA6 are potent KIT inhibitors." Cell Death Dis **10**(4): 300.

Mahat, R. K., N. Singh, M. Arora and V. Rathore (2019). "Health risks and interventions in prediabetes: A review." Diabetes Metab Syndr **13**(4): 2803-2811.

Mahendran, Y., J. Vangipurapu, H. Cederberg, A. Stancakova, J. Pihlajamaki, P. Soininen, A. J. Kangas, J. Paananen, M. Civelek, N. K. Saleem, P. Pajukanta, A. J. Lusis, L. L. Bonnycastle, M. A. Morken, F. S. Collins, K. L. Mohlke, M. Boehnke, M. Ala-Korpela, J. Kuusisto and M. Laakso (2013). "Association of ketone body levels with hyperglycemia and type 2 diabetes in 9,398 Finnish men." Diabetes **62**(10): 3618-3626.

Manning, B. D. (2010). "Insulin signaling: inositol phosphates get into the Akt." Cell **143**(6): 861-863.

Maurel, M., E. Chevet, J. Tavernier and S. Gerlo (2014). "Getting RIDD of RNA: IRE1 in cell fate regulation." Trends Biochem Sci **39**(5): 245-254.

Merksamer, P. I., A. Trusina and F. R. Papa (2008). "Real-time redox measurements during endoplasmic reticulum stress reveal interlinked protein folding functions." Cell **135**(5): 933-947.

Milanski, M., G. Degasperi, A. Coope, J. Morari, R. Denis, D. E. Cintra, D. M. Tsukumo, G. Anhe, M. E. Amaral, H. K. Takahashi, R. Curi, H. C. Oliveira, J. B. Carvalheira, S. Bordin, M. J. Saad and L. A. Velloso (2009). "Saturated fatty acids produce an inflammatory response predominantly through the activation of TLR4 signaling in hypothalamus: implications for the pathogenesis of obesity." J Neurosci **29**(2): 359-370.

Morita, S., S. A. Villalta, H. C. Feldman, A. C. Register, W. Rosenthal, I. T. Hoffmann-Petersen, M. Mehdizadeh, R. Ghosh, L. Wang, K. Colon-Negron, R. Meza-Acevedo, B.

J. Backes, D. J. Maly, J. A. Bluestone and F. R. Papa (2017). "Targeting ABL-IRE1alpha Signaling Spares ER-Stressed Pancreatic beta Cells to Reverse Autoimmune Diabetes." Cell Metab **25**(4): 883-897 e888.

Morita, S., S. A. Villalta, H. C. Feldman, A. C. Register, W. Rosenthal, I. T. Hoffmann-Petersen, M. Mehdizadeh, R. Ghosh, L. Wang, K. Colon-Negron, R. Meza-Acevedo, B. J. Backes, D. J. Maly, J. A. Bluestone and F. R. Papa (2017). "Targeting ABL-IRE1alpha Signaling Spares ER-Stressed Pancreatic beta Cells to Reverse Autoimmune Diabetes." Cell Metab **25**(5): 1207.

Nishitoh, H., A. Matsuzawa, K. Tobiume, K. Saegusa, K. Takeda, K. Inoue, S. Hori, A. Kakizuka and H. Ichijo (2002). "ASK1 is essential for endoplasmic reticulum stress-induced neuronal cell death triggered by expanded polyglutamine repeats." Genes Dev **16**(11): 1345-1355.

Oh, Y. S., G. D. Bae, D. J. Baek, E. Y. Park and H. S. Jun (2018). "Fatty Acid-Induced Lipotoxicity in Pancreatic Beta-Cells During Development of Type 2 Diabetes." Front Endocrinol (Lausanne) **9**: 384.

Ozcan, U., Q. Cao, E. Yilmaz, A. H. Lee, N. N. Iwakoshi, E. Ozdelen, G. Tuncman, C. Gorgun, L. H. Glimcher and G. S. Hotamisligil (2004). "Endoplasmic reticulum stress links obesity, insulin action, and type 2 diabetes." Science **306**(5695): 457-461.

Ozcan, U., E. Yilmaz, L. Ozcan, M. Furuhashi, E. Vaillancourt, R. O. Smith, C. Z. Gorgun and G. S. Hotamisligil (2006). "Chemical chaperones reduce ER stress and restore glucose homeostasis in a mouse model of type 2 diabetes." Science **313**(5790): 1137-1140.

Papa, F. R., C. Zhang, K. Shokat and P. Walter (2003). "Bypassing a kinase activity with an ATP-competitive drug." Science **302**(5650): 1533-1537.

Puri, P., F. Mirshahi, O. Cheung, R. Natarajan, J. W. Maher, J. M. Kellum and A. J. Sanyal (2008). "Activation and dysregulation of the unfolded protein response in nonalcoholic fatty liver disease." Gastroenterology **134**(2): 568-576.

Puri, S., N. Roy, H. A. Russ, L. Leonhardt, E. K. French, R. Roy, H. Bengtsson, D. K. Scott, A. F. Stewart and M. Hebrok (2018). "Replication confers beta cell immaturity." Nat Commun **9**(1): 485.

Robertson, R. P., J. Harmon, P. O. Tran and V. Poitout (2004). "Beta-cell glucose toxicity, lipotoxicity, and chronic oxidative stress in type 2 diabetes." Diabetes **53 Suppl 1**: S119-124.

Robertson, R. P., J. Harmon, P. O. Tran, Y. Tanaka and H. Takahashi (2003). "Glucose toxicity in beta-cells: type 2 diabetes, good radicals gone bad, and the glutathione connection." Diabetes **52**(3): 581-587.

Ron, D. and P. Walter (2007). "Signal integration in the endoplasmic reticulum unfolded protein response." Nat Rev Mol Cell Biol **8**(7): 519-529.

Salvado, L., X. Palomer, E. Barroso and M. Vazquez-Carrera (2015). "Targeting endoplasmic reticulum stress in insulin resistance." Trends Endocrinol Metab **26**(8): 438-448.

Sanders, F. W. and J. L. Griffin (2016). "De novo lipogenesis in the liver in health and disease: more than just a shunting yard for glucose." Biol Rev Camb Philos Soc **91**(2): 452-468.

Sarbassov, D. D., D. A. Guertin, S. M. Ali and D. M. Sabatini (2005). "Phosphorylation and regulation of Akt/PKB by the rictor-mTOR complex." Science **307**(5712): 1098-1101.

Scheuner, D., B. Song, E. McEwen, C. Liu, R. Laybutt, P. Gillespie, T. Saunders, S. Bonner-Weir and R. J. Kaufman (2001). "Translational control is required for the unfolded protein response and in vivo glucose homeostasis." Mol Cell **7**(6): 1165-1176.

Sharma, R. B. and L. C. Alonso (2014). "Lipotoxicity in the pancreatic beta cell: not just survival and function, but proliferation as well?" Curr Diab Rep **14**(6): 492.

Shen, X., R. E. Ellis, K. Lee, C. Y. Liu, K. Yang, A. Solomon, H. Yoshida, R. Morimoto, D. M. Kurnit, K. Mori and R. J. Kaufman (2001). "Complementary signaling pathways

regulate the unfolded protein response and are required for C. elegans development." Cell **107**(7): 893-903.

Thamsen, M., R. Ghosh, V. C. Auyeung, A. Brumwell, H. A. Chapman, B. J. Backes, G. Perara, D. J. Maly, D. Sheppard and F. R. Papa (2019). "Small molecule inhibition of IRE1alpha kinase/RNase has anti-fibrotic effects in the lung." PLoS One **14**(1): e0209824.

Tirasophon, W., A. A. Welihinda and R. J. Kaufman (1998). "A stress response pathway from the endoplasmic reticulum to the nucleus requires a novel bifunctional protein kinase/endoribonuclease (Ire1p) in mammalian cells." Genes Dev **12**(12): 1812-1824.

Tirosh, A., I. Shai, R. Bitzur, I. Kochba, D. Tekes-Manova, E. Israeli, T. Shochat and A. Rudich (2008). "Changes in triglyceride levels over time and risk of type 2 diabetes in young men." Diabetes Care **31**(10): 2032-2037.

Trusina, A., F. R. Papa and C. Tang (2008). "Rationalizing translation attenuation in the network architecture of the unfolded protein response." Proc Natl Acad Sci U S A **105**(51): 20280-20285.

Upton, J. P., L. Wang, D. Han, E. S. Wang, N. E. Huskey, L. Lim, M. Truitt, M. T. McManus, D. Ruggero, A. Goga, F. R. Papa and S. A. Oakes (2012). "IRE1alpha cleaves select microRNAs during ER stress to derepress translation of proapoptotic Caspase-2." Science **338**(6108): 818-822.

Urano, F., X. Wang, A. Bertolotti, Y. Zhang, P. Chung, H. P. Harding and D. Ron (2000). "Coupling of stress in the ER to activation of JNK protein kinases by transmembrane protein kinase IRE1." Science **287**(5453): 664-666.

Valenti, L., R. Rametta, P. Dongiovanni, M. Maggioni, A. L. Fracanzani, M. Zappa, E. Lattuada, G. Roviaro and S. Fargion (2008). "Increased expression and activity of the transcription factor FOXO1 in nonalcoholic steatohepatitis." Diabetes **57**(5): 1355-1362.

van Anken, E. and I. Braakman (2005). "Versatility of the endoplasmic reticulum protein folding factory." Crit Rev Biochem Mol Biol **40**(4): 191-228.

Vembar, S. S. and J. L. Brodsky (2008). "One step at a time: endoplasmic reticulum-associated degradation." Nat Rev Mol Cell Biol **9**(12): 944-957.

Volmer, R. and D. Ron (2015). "Lipid-dependent regulation of the unfolded protein response." Curr Opin Cell Biol **33**: 67-73.

Walter, P. and D. Ron (2011). "The unfolded protein response: from stress pathway to homeostatic regulation." Science **334**(6059): 1081-1086.

Wang, L., B. G. Perera, S. B. Hari, B. Bhhatarai, B. J. Backes, M. A. Seeliger, S. C. Schurer, S. A. Oakes, F. R. Papa and D. J. Maly (2012). "Divergent allosteric control of the IRE1alpha endoribonuclease using kinase inhibitors." Nat Chem Biol **8**(12): 982-989.

Wang, X. Z., H. P. Harding, Y. Zhang, E. M. Jolicoeur, M. Kuroda and D. Ron (1998). "Cloning of mammalian Ire1 reveals diversity in the ER stress responses." EMBO J **17**(19): 5708-5717.

Wang, X. Z., M. Kuroda, J. Sok, N. Batchvarova, R. Kimmel, P. Chung, H. Zinszner and D. Ron (1998). "Identification of novel stress-induced genes downstream of chop." EMBO J **17**(13): 3619-3630.

Wang, Y., J. Shen, N. Arenzana, W. Tirasophon, R. J. Kaufman and R. Prywes (2000). "Activation of ATF6 and an ATF6 DNA binding site by the endoplasmic reticulum stress response." J Biol Chem **275**(35): 27013-27020.

Weston, C. R. and R. J. Davis (2007). "The JNK signal transduction pathway." Curr Opin Cell Biol **19**(2): 142-149.

Whittaker, L., C. Hao, W. Fu and J. Whittaker (2008). "High-affinity insulin binding: insulin interacts with two receptor ligand binding sites." Biochemistry **47**(48): 12900-12909.

Ye, J., R. B. Rawson, R. Komuro, X. Chen, U. P. Dave, R. Prywes, M. S. Brown and J. L. Goldstein (2000). "ER stress induces cleavage of membrane-bound ATF6 by the same proteases that process SREBPs." Mol Cell **6**(6): 1355-1364.

Yoshida, H., T. Matsui, A. Yamamoto, T. Okada and K. Mori (2001). "XBP1 mRNA is induced by ATF6 and spliced by IRE1 in response to ER stress to produce a highly active transcription factor." Cell **107**(7): 881-891.

Zhang, K. and R. J. Kaufman (2006). "The unfolded protein response: a stress signaling pathway critical for health and disease." Neurology **66**(2 Suppl 1): S102-109.

Zhang, L., C. Zhang and A. Wang (2016). "Divergence and Conservation of the Major UPR Branch IRE1-bZIP Signaling Pathway across Eukaryotes." Sci Rep **6**: 27362.

Zinszner, H., M. Kuroda, X. Wang, N. Batchvarova, R. T. Lightfoot, H. Remotti, J. L. Stevens and D. Ron (1998). "CHOP is implicated in programmed cell death in response to impaired function of the endoplasmic reticulum." Genes Dev **12**(7): 982-995.

Publishing Agreement

It is the policy of the University to encourage the distribution of all theses, dissertations, and manuscripts. Copies of all UCSF theses, dissertations, and manuscripts will be routed to the library via the Graduate Division. The library will make all theses, dissertations, and manuscripts accessible to the public and will preserve these to the best of their abilities, in perpetuity.

Please sign the following statement:

I hereby grant permission to the Graduate Division of the University of California, San Francisco to release copies of my thesis, dissertation, or manuscript to the Campus Library to provide access and preservation, in whole or in part, in perpetuity.

Kevin A. Colón-Negrón
Author Signature

08/27/2019
Date